

# TracerX: Dynamic Symbolic Execution with Interpolation

JOXAN JAFFAR, National University of Singapore  
 RASOOL MAGHAREH, National University of Singapore  
 SANGHARATNA GODBOLEY, National University of Singapore  
 XUAN-LINH HA, National University of Singapore

Dynamic Symbolic Execution is an important method for the testing of programs. An important system on DSE is KLEE [Cadare et al. 2008a] which inputs a C/C++ program annotated with symbolic variables, compiles it into LLVM, and then emulates the execution paths of LLVM using a specified backtracking strategy. The major challenge in symbolic execution is *path explosion*. The method of *abstraction learning* [Jaffar et al. 2009; McMillan 2010, 2014] has been used to address this. The key step here is the computation of an *interpolant* to represent the learnt abstraction.

In this paper, we present a new interpolation algorithm and implement it on top of the KLEE system. The main objective is to address the path explosion problem in pursuit of *code penetration*: to prove that a target program point is either reachable or unreachable. That is, our focus is verification. We show that despite the overhead of computing interpolants, the *pruning* of the symbolic execution tree that interpolants provide often brings significant overall benefits. We then performed a comprehensive experimental evaluation against KLEE, as well as against one well-known system that is based on Static Symbolic Execution, CBMC [Clarke et al. 2004]. Our primary experiment shows code penetration success at a new level, particularly so when the target is hard to determine. A secondary experiment shows that our implementation is competitive for testing.

Additional Key Words and Phrases: Symbolic Execution, Software Testing, Interpolation

## 1 INTRODUCTION

Symbolic execution (SE) has emerged as an important method to reason about programs, in both verification and testing. By reasoning about inputs as symbolic entities, its fundamental advantage over traditional black-box testing, which uses concrete inputs, is simply that it has better *coverage* of *program paths*. In particular, *dynamic symbolic execution* (DSE), where the execution space is explored *path-by-path*, has been shown effective in systems such as DART [Godefroid et al. 2005], CUTE [Sen et al. 2005] and KLEE [Cadare et al. 2008a]<sup>1</sup>.

A key advantage of DSE is that by examining a single path, the analysis can be both precise (for example, capturing intricate details such as the state of the cache micro-architecture), and efficient (for example, the constraint solver often needs to deal with path constraints that are aggregated into a single conjunction). Another advantage is the possibility of reasoning about system or library functions which we can execute but not analyze, as in the method of *concolic testing* CUTE [Sen et al. 2005]. Yet another advantage is the ability to realize a *search strategy* in the path exploration, such as in a random, depth-first, or breadth-first manner, or in a manner determined by the program structure. However, the key disadvantage of DSE is that the number of program paths is in general exponential in the program size, and most available implementations of DSE do not employ a general technique to prune away some paths. Indeed, a recent paper [Avgerinos et al. 2016] describes that DSE “traditionally forks off two executors at the same line,

<sup>1</sup>It is not universally agreed that KLEE is a DSE system, but we follow the terminology in two recent CACM articles [Avgerinos et al. 2016; Cadare and Sen 2013].

Authors’ addresses: Joxan Jaffar, National University of Singapore, joxan@comp.nus.edu.sg; Rasool Maghareh, National University of Singapore, rasool@comp.nus.edu.sg; Sangharatna Godbole, National University of Singapore, sanghara@comp.nus.edu.sg; Xuan-Linh Ha, National University of Singapore, haxl@comp.nus.edu.sg.

which remain subsequently forever independent”, clearly suggesting that the DSE processing of different paths have no symbiosis.

A variant of symbolic execution is that of Static Symbolic Execution (SSE), see e.g. [Avgerinos et al. 2016; Khurshid et al. 2003]. The general idea is that the symbolic execution tree is encoded as a single logic formula whose treatment can be outsourced to an SMT solver [De Moura et al. 2002]. The solver then deals with what is essentially a huge disjunctive formula. Clearly, there are some limitations to this approach as compared with DSE, for example, the loop bounds, including nested loops, must be pre-specified. However, SSE has a huge advantage over (non-pruning) DSE: its SMT solver can use the optimization method of *conflict directed clause learning* (CDCL) [Marques-Silva and Sakallah 1999]. See e.g. Section 3.4 of [de Moura and Bjørner 2008] on how the SMT solver Z3 exploits CDCL. Essentially, CDCL enables “pruning” in the exploration process of the solver.

In this paper, our primary objective is to address the path explosion problem in DSE. More specifically, we wish to perform a path-by-path exploration of DSE to enjoy its benefits, but we include a *pruning mechanism* so that path generation can be eliminated if the path generated so far is guaranteed not to violate the stated safety conditions. Toward this goal, we employ the method of *abstraction learning* [Jaffar et al. 2009], which is more popularly known as *lazy annotations* (LA) [McMillan 2010, 2014]. The core feature of this method is the use of *interpolation*, which serves to generalize the context of a node in the symbolic execution tree with an approximation of the weakest precondition of the node. This method has been implemented in the TRACER system [Jaffar et al. 2012, 2011] which was the first system to demonstrate DSE with pruning. While TRACER was able to perform bounded verification and testing on many examples, it could not accommodate industrial programs that often dynamically manipulate the heap memory. Instead, TRACER was primarily used to evaluate new algorithms in verification, analysis, and testing, e.g., [Chu and Jaffar 2012; Chu et al. 2016; Jaffar et al. 2013].

The main contribution of this paper is the design and implementation of a new interpolation algorithm, and integration into the KLEE system. In our primary experiment, we compare against KLEE. In a secondary experiment, we consider the related area of Static Symbolic Execution (SSE). The reason is that, while SSE is generally considered as significantly different from DSE, SSE is a competitor to DSE because they both address many common analysis problems.

Our main experimental result is that our algorithm leads in *code penetration*: given a target, which is essentially a designated program point, can one prove that the target is reachable, or prove that the target is unreachable. Thus our algorithm is more aligned with verification rather than testing. We suggest two driving applications for such verification. One is to confirm/deny an “alarm” from a static analysis; an alarm is a target for which there is a plausible reason for it to be a true bug. Another application is dead code detection. Penetration addresses both these questions.

Given that our algorithm is relatively heavy-weight, it is expected that for some examples, the overhead is not worth it. We show firstly that our implemented system performs well on a large benchmark suite. We then considered a subset of the original targets called *hard targets*. These are obtained by filtering out targets that can be proved easily by state-of-the-art methods: vanilla symbolic execution for reachable targets, and static analysis for unreachable targets. We then show that for the remaining (hard) targets, the performance gap widens.

We then performed a secondary experimental evaluation for testing. Here we followed the setup of the TEST-COMP competition by evaluating on *bug finding* (given a set of targets, find one) and *code coverage* (where all program blocks are targets, and to find as many as possible). In this secondary experiment, we show that our implementation is competitive.

## 2 A MOTIVATING EXAMPLE

Consider the shortest path problem in graphs. See Fig. 1 where we assume the graph has edges, where each of which has a “distance”. The edges point from a lower-numbered vertex to a higher one. The variable  $d$  computes the distance between nodes 1 and  $N$  via the traversed path. In the end, we want to know if  $d \geq BOUND$  for some given constant  $BOUND$ . Symbolic execution on this program (where the variable node is symbolic) will traverse all paths, and therefore will be able to check the bound. Then, by iteratively executing symbolic execution with various values of  $BOUND$ , we can solve the shortest path problem.

```
#define N ...
int graph[N+1][N+1] = { ... };
int node = 1, d = 0;
while (node < N) {
    int next = new symbolic variable;
    for (i = node + 1; i < N; i++)
        if (next == i) d += graph[node][next]; break;
    node = next;
}
assert (d >= BOUND);
```

Fig. 1. Motivating Example 1

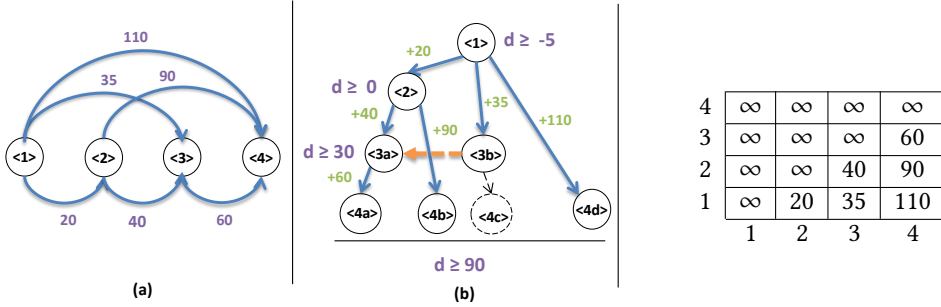


Fig. 2. Example with Interpolation (a) Graph (b) Symbolic Execution Tree

Table 1. Adjacency Matrix

*Example 2.1.* Consider the example graph in Fig. 2 (a) and its respective adjacency matrix in Table 1. The execution tree of the program from Fig. 1 is presented in Fig. 2(b). The program points <1> and <4> represent the source and destination nodes. The program points using the same number, e.g. <3a> and <3b>, identify different visits to the same program point. Now assume we want to ensure that the distance between nodes 1 and 4 is greater than  $BOUND = 90$  at the end. A basic DSE tool will traverse all the paths in the execution tree if there is no pruning. There would be a problem for this example because the number of the paths is exponential in  $N$ .

Now we will demonstrate how our approach can prune the execution tree. Since our approach is built on top of DSE, all the program points in the loop iterations possess the same program point. Hence, we can compare the states in different iterations and prune them when possible. Consider the leftmost path <1>, <2>, <3a>, and <4a>. At the end of this path, since the distance  $d$  is 120, the assertion is not violated and an *interpolant* is stored at <3>:  $d \geq 30$ . This interpolant represents the *weakest precondition* at <3> which satisfies the assertion. It is computed by updating the safety property  $d \geq 90$  with the update on  $d$  between nodes <3a>, and <4a>:  $d = d + 60$ . Next,

this interpolant is passed to the parent node  $\langle 2 \rangle$  considering the update on the variable  $d$  between  $\langle 2 \rangle$  and  $\langle 3a \rangle$ :  $d \geq -10$ .

Backtracking back to  $\langle 2 \rangle$ , we now consider the second path  $\langle 1 \rangle, \langle 2 \rangle, \langle 4b \rangle$ . Here again, the assertion is not violated and an interpolant is passed to node  $\langle 2 \rangle$  considering the update on  $d$  between  $\langle 2 \rangle$  and  $\langle 4b \rangle$ :  $d \geq 0$ . Now the intersection of the two interpolants received from the successor nodes of  $\langle 2 \rangle$  is stored as the interpolant of  $\langle 2 \rangle$ :  $d \geq 0$ .

Moving on, this interpolant is updated and sent to the parent node  $\langle 1 \rangle$ :  $d \geq -20$ . Next, the path  $\langle 1 \rangle, \langle 3b \rangle$ , and  $\langle 4c \rangle$  is traversed. Here, at node  $\langle 3b \rangle$  the distance is  $d = 35$ , and the interpolant stored at  $\langle 3a \rangle$  ( $d \geq 30$ ) can be used to *prune* this node. Note importantly that node  $\langle 3a \rangle$  was visited in the third iteration of the loop (in the program from Fig. 1) and node  $\langle 3b \rangle$  is visited in the second iteration. Here, the pruning is sound since both program points are on the same node in the graph (node 3) and the state at  $\langle 3b \rangle$  satisfies the respective weakest precondition interpolant.

This subsumed node is considered to have an interpolant,  $d \geq 30$ , that which subsumed it. This is passed to node  $\langle 1 \rangle$ :  $d \geq -5$ . Finally, the last path  $\langle 1 \rangle, \langle 4d \rangle$  is traversed and since the assertion is not violated an interpolant is passed to node  $\langle 1 \rangle$ :  $d \geq -20$ . Now the three interpolants passed to  $\langle 1 \rangle$ ,  $d \geq -20$  from  $\langle 2 \rangle$ ,  $d \geq -5$  from  $\langle 3b \rangle$ ,  $d \geq -20$  from  $\langle 4c \rangle$ , is combined as a conjunction and stored as an interpolant at  $\langle 1 \rangle$ :  $d \geq -5$ .

This interpolant at the root infers that all values of  $d$  greater than or equal  $-5$  will not violate the assertion. From this, we can infer that if the condition in the assertion had been  $d \geq 95$ , it would still have not been violated. That is, we can, in fact, conclude that the shortest path between nodes 1 and 4 in the graph is 95, a tighter bound than what we started with.  $\square$

For this example, our implementation can deal with 1000 nodes, while CBMC and KLEE tops out at 100 and 25 respectively.

### 3 BACKGROUND: SYMBOLIC EXECUTION

We formalize dynamic symbolic execution (DSE) for a toy programming language. The variables in a program are denoted  $Vars$ . Other than the program variables  $Vars_p$ , there are also *symbolic* variables  $Vars_s$ . A basic statement is the assignment,  $var = exp$  where  $exp$  is some arithmetic or boolean expression. Another basic statement is  $assume(exp)$  where  $exp$  is a boolean expression. Note that “assertions” can be modeled by  $assume()$  statements coupled with a distinguished statement representing error.

For brevity, we omit other statements, e.g. functions, memory operations like arrays, malloc, etc. Extension to cover these instructions would be routine. In general, we follow the semantics used by KLEE for these instructions. We will further discuss some implementation details for these instructions in Section 5.2.

We model a program  $P$  by a transition system: a tuple  $\langle \Sigma, \ell_{start}, \longrightarrow \rangle$  where  $\Sigma$  is the set of program points and  $\ell_{start} \in \Sigma$  is the *unique* initial program point. Let  $\longrightarrow \subseteq \Sigma \times \Sigma \times Stmts$ , where  $Stmts$  is the set of program statements, be the transition relation that relates a state to its (possible) successors by executing the statements. We shall use  $\ell \xrightarrow{stmt} \ell'$  to denote a transition relation from  $\ell \in \Sigma$  to  $\ell' \in \Sigma$  executing the statement  $stmt \in Stmts$ .

**Definition 3.1 (Symbolic State).** A symbolic state  $s$  is a tuple  $\langle \ell, \Pi \rangle$ , where  $\ell \in \Sigma$  is the current program point, and the constraint store (or “context”)  $\Pi$  is a first-order formula over symbolic variables  $Vars_s$  and program variables  $Vars_p$ .  $\square$

The *evaluation*  $\llbracket x = exp \rrbracket_{\Pi}$  of an expression  $exp$  with the constraint store  $\Pi$  is defined in the standard way by  $\Pi[x/exp]$ . Similarly, the evaluation  $\llbracket assume(exp) \rrbracket_{\Pi}$  is defined by  $\Pi \wedge exp$ . (Note that our expressions have no *side-effects*.) The notion of evaluation is extended for a set of constraints in an intuitive way. The evaluation of the constraint store of a state is denoted by  $\llbracket s \rrbracket$ .

A symbolic state  $s \equiv \langle \ell, \Pi \rangle$  is called *infeasible* if  $\llbracket s \rrbracket$  is unsatisfiable. Otherwise, the state is called *feasible*; symbolic execution is possible from a feasible state only.

**Definition 3.2 (Transition Step).** Given a feasible symbolic state  $s \equiv \langle \ell, \Pi \rangle$ , and a transition system  $\langle \Sigma, \ell_{\text{start}}, \longrightarrow \rangle$  the symbolic execution of transition  $\ell \xrightarrow{\text{stmt}} \ell'$  returns a *successor state*  $\langle \ell', \Pi' \rangle$  where  $\Pi'$  is computed via  $\llbracket \text{stmt} \rrbracket_{\Pi}$ .  $\square$

Let  $s_0 \equiv \langle \ell_{\text{start}}, \text{true} \rangle$  be the *initial* symbolic state. A *symbolic path*  $s_0 \rightarrow s_1 \cdots \rightarrow s_m$  denoted by  $\vec{s}$  is a sequence of symbolic states such that  $\forall 1 \leq i \leq m, s_i$  is a *successor* of  $s_{i-1}$ . We can now define *symbolic exploration* as the process of constructing a *Symbolic Execution Tree* (SET) rooted at  $s_0$ . Following some *search strategy*, the order in which the nodes are constructed can be different. For bounded verification and testing, we assume that the tree depth is bounded. Note that only one of our program statements, *assume*( $e$ ), is a “branch”. This means that in a SET, a state has at most two successors.

The reachability of an error statement indicates a *bug*. Symbolic execution typically stops the path and generates a *failed* test case witnessing that bug. On the other hand, a path *safely* terminates if we reach a *halt* statement, and we also generate a *passed* test case. We prove a program is *safe* by showing that no error statement is reached. A subtree is called *safe* if no error statement is reached from its root.

### 3.1 Symbolic Execution with Interpolation

We now present a formulation of the method of dynamic symbolic execution with interpolation (DSEI) [Jaffar et al. 2009; McMillan 2010]. The essential idea, in brief, is this. In exploring the SET, an *interpolant*  $\Psi$  of a state  $s$  is an *abstraction* of it which ensures the safety of the subtree rooted at that state. In other words, if we continue the execution with  $\Psi$  instead of  $s$ , we will *not* reach any error. Thus upon encountering a state  $\bar{s}$  of the same program point as  $s$ , i.e.,  $s$  and  $\bar{s}$  have the same set of emanating transitions, if  $\bar{s} \models \Psi$ , then continuing the execution from  $\bar{s}$  will not lead to an error. Consequently, we can prune the subtree rooted at  $\bar{s}$ .

DSEI is a *top-down* method, because it traverses the SET from the root, and is also *bottom-up* because it propagates formulas backward from the end of a path in the SET. Before proceeding with describing DSEI, let us briefly argue that using just a bottom-up approach using the concept of *weakest precondition*, is not practical. Before proceeding, consider using classic weakest preconditions, which operate on program fragments, not paths. The main disadvantage here is that being entirely bottom-up, the computed precondition at a program point is *agnostic* to the *context* of the states which reach that program point.

In contrast, DSEI performs a top-down depth-first search of the state space, path by path. For each path, it computes a *path interpolant*. This is where DSEI is bottom-up. For each subtree, it computes a *tree interpolant* being the conjunction of all of the path interpolants from within the subtree.

Now, we describe how to compute a path interpolant. This is computed recursively in a bottom-up manner. Consider  $\vec{s}$  being a sequence of states,  $\vec{s}.\text{stmt}$  to denote the sequence  $\vec{s}$  appended with a state  $s$  where  $s$  is obtained by executing *stmt* from the last state in  $\vec{s}$ , and the postcondition *post*, the function  $\text{INTP}()$  computes the path-based weakest precondition interpolant. In case  $\vec{s}$  is the empty sequence, denoted by  $\epsilon$ , then  $\vec{s}.\text{stmt}$  is simply the state obtained by executing *stmt* on the initial state.

**Definition 3.3 (Path-based Weakest Precondition).** Path-based weakest precondition is the weakest precondition of a symbolic path  $\vec{s}$  with respect to a postcondition *Post*. This is formalized in Fig. 3.  $\square$

(1a)	$\text{INTP}(\epsilon, \Psi)$	$= \Psi$
(2a)	$\text{INTP}(\vec{s}, x = e, \Psi)$	$= \text{INTP}(\vec{s}, \Psi[x/e])$
(3a)	$\text{INTP}(\vec{s}, \text{assume}(e), \text{false})$	$= \text{INTP}(\vec{s}, \neg e)$
(4a)	$\text{INTP}(\vec{s}, \text{assume}(e), \Psi)$	$= \text{INTP}(\vec{s}, e \implies \Psi)$

Fig. 3. Path-Based Weakest Precondition

See Fig. 3. Rule (1a) and (2a) are the base cases and their process is well-understood. We simply present an example. Suppose  $x = e$  were  $x = x + 5$  and  $\Psi$  were  $x < 7$ , then the weakest precondition is  $x < 2$ . In general, for an assignment of a variable to an expression  $e$ , say  $x = x + e$ , the weakest precondition wrt. to  $\Psi$  is  $\Psi[x/x + e]$ , i.e. the formula obtained from  $\Psi$  by simultaneously replacing all its occurrences of  $x$  with  $x + e$ .

Next, rule (3a) addresses the case that a node is infeasible in the SET. Finally, we should highlight that in rule (4a), the interpolant  $e \implies \Psi$  still generates a *disjunction*. Consequently, the path-based weakest precondition, in general, may be a very large *disjunction*, exponential in the program length.

*Example 3.4.* Consider the example in Fig. 4, where  $b[i]$  is a symbolic bit-vector,  $Pre$  an unspecified Boolean condition on the bit-vector representing the *precondition*, and  $Post$  an unspecified Boolean condition on any variables, representing the *postcondition*.

```

bool b[N];
assume(Pre);
(1) if (b[1])  $\kappa_1 = 1$ ; else  $\kappa_1 = -1$ ;
(2) if (b[2])  $\kappa_2 = 1$ ; else  $\kappa_2 = -1$ ;
...
(N) if (b[N])  $\kappa_n = 1$ ; else  $\kappa_n = -1$ ;
assert(Post);

```

Fig. 4. Example

Suppose  $N = 3$ , and  $Pre$  implies  $b[1] == b[2] \wedge b[2] == b[3]$ .

The classic weakest precondition of the program with postcondition  $Post$  is a disjunction of 8 distinct formulas, each of which is (a) an assignment of specific bit values to the variables  $b[i]$  conjoined with (b) a formula representing the propagation of the postcondition  $Post$  through the  $\kappa_i$  assignments corresponding to the  $b[i]$  assignments in (a). These 8 formulas are

$$\begin{aligned}
&b[1] == 1 \wedge b[2] == 1 \wedge b[3] == 1 \wedge Post[\kappa_1/1, \kappa_2/1, \kappa_3/1] \\
&b[1] == 1 \wedge b[2] == 1 \wedge b[3] == 0 \wedge Post[\kappa_1/1, \kappa_2/1, \kappa_3/-1] \\
&b[1] == 1 \wedge b[2] == 0 \wedge b[3] == 1 \wedge Post[\kappa_1/1, \kappa_2/-1, \kappa_3/1] \\
&b[1] == 1 \wedge b[2] == 0 \wedge b[3] == 0 \wedge Post[\kappa_1/1, \kappa_2/-1, \kappa_3/-1] \\
&b[1] == 0 \wedge b[2] == 1 \wedge b[3] == 1 \wedge Post[\kappa_1/-1, \kappa_2/1, \kappa_3/1] \\
&b[1] == 0 \wedge b[2] == 1 \wedge b[3] == 0 \wedge Post[\kappa_1/-1, \kappa_2/1, \kappa_3/-1] \\
&b[1] == 0 \wedge b[2] == 0 \wedge b[3] == 1 \wedge Post[\kappa_1/-1, \kappa_2/-1, \kappa_3/1] \\
&b[1] == 0 \wedge b[2] == 0 \wedge b[3] == 0 \wedge Post[\kappa_1/-1, \kappa_2/-1, \kappa_3/-1]
\end{aligned}$$

By way of comparison, in the *path-based* weakest precondition, 6 of 8 of these formulas would be unsatisfiable. Thus, the *path-based* weakest precondition, after simplification, would be the following 2 formulas at (1).

$$\begin{aligned}
&b[1] == 1 \wedge b[2] == 1 \wedge b[3] == 1 \wedge Post[\kappa_1/1, \kappa_2/1, \kappa_3/1] \\
&b[1] == 0 \wedge b[2] == 0 \wedge b[3] == 0 \wedge Post[\kappa_1/-1, \kappa_2/-1, \kappa_3/-1]. \quad \square
\end{aligned}$$

```

DSEI(s) { // returns a tree interpolant ( $\Psi$ )
(1) if (UNSAT( $\llbracket s \rrbracket$ )) return false; // Infeasible node
(2) if ( $s \models \Psi$ ) return  $\Psi$ ;
(3) if (s is terminal) {
(4)   if ( $s \models \Phi$ ) return  $\Phi$ ; //  $\Phi$  is the safety property
(5)   else return error; // Counter-example
(6) }
(7)  $\Psi' = \Psi'' = \text{true}$ ;
(8) if there is a transition  $s \xrightarrow{\text{stmt}} s'$  {
(9)    $\Psi = \text{DSEI}(s')$ ;
(10)  if ( $\Psi \neq \text{false}$  and  $\Psi \neq \text{error}$ )  $\Psi' = \text{BACKPROP}(s, \text{stmt}, \Psi)$ ;
(11)  else return  $\Psi$ ;
(12) }
(13) if there is another transition  $s \xrightarrow{\text{stmt}' } s''$  {
(14)   $\Psi = \text{DSEI}(s'')$ ;
(15)  if ( $\Psi \neq \text{false}$  and  $\Psi \neq \text{error}$ )  $\Psi'' = \text{BACKPROP}(s, \text{stmt}', \Psi)$ ;
(16)  else return  $\Psi$ ;
(17) }
(18) return  $\Psi' \wedge \Psi''$ ;
(19) }

```

Fig. 5. The DSEI Algorithm

The idea here is that classic weakest precondition, as it traverses is agnostic to precondition, and there it essentially traverses every path through the program. Only at the end it is known that only 2 of the 8 formulas generated cover the precondition.

We finally comment that in the path-based weakest precondition, though it has only two formulas, this still is a *disjunction*. In the next two sections, we present our algorithm which *approximates* the weakest path-based weakest precondition with a single *conjunction*.

#### 4 THE MAIN ALGORITHM

The overall structure of our idealized algorithm is in Fig. 5, where it processes a symbolic execution tree (SET) via DSEI. The function DSEI receives a symbolic state  $s$  which represents a node from the SET. It then processes the subtree beneath the node and returns an interpolant  $\Psi$ . If  $s$  is safe, i.e. all paths from  $s$  do not violate the assertion, then  $\Psi$  is an *interpolant* storing a generalization of the state  $s$ . If, on the other hand,  $s$  is unsafe, i.e. there is one path from  $s$  that violates assertion, then  $\Psi$  is error.

The DSEI( $s$ ) function first checks if a state is infeasible (line (1)). The return value is simply *false* (as the interpolant).

At lines (3)-(6) (when  $s$  is a terminal node, i.e. it has no successors), it is checked if  $s$  is safe, then  $\Phi$  is returned as an interpolant for the *safe* terminal node. Otherwise, a counter-example is found and error is returned.

Next, in lines (8)-(12), the DSEI function is recursively called on  $s'$  which is a successor node of  $s$  via the transition  $s \xrightarrow{\text{stmt}} s'$ . After the call is returned (line (10)), it is checked if the interpolant  $\Psi$  is *false* or error. If so, *false* or error is returned (line (11)).

The key element of the algorithm is in line (10), where the BACKPROP( $s, \text{stmt}, \Psi$ ) function returns  $\Psi'$ , a practical estimation of the *weakest precondition* of the statement  $\text{stmt}$  wrt. a postcondition  $\Psi$ . Note importantly that here we cannot use the *path-based* weakest precondition from Section 3.1,

since it generates a disjunctive interpolant. In Section 5, we present the *interpolation algorithm* of the BACKPROP function.

Similarly, in lines (13)-(17), if another transition  $s \xrightarrow{\text{stmt}'} s''$  exists, the successor node  $s''$  is processed and the interpolant  $\Psi''$  is computed.

Finally, the *tree interpolant* is returned in line (20) which is the conjunction of  $\Psi'$  and  $\Psi''$ . Note here that  $\Psi' \wedge \Psi''$  contains a condition which while not violated, ensures all paths within the subtree beneath  $s$  will not lead to a violation of the safety property  $\Phi$ .

The key to performance is the subsumption step in line (2). Here  $\Psi$  contains the interpolant generated from processing a similar node in the SET, i.e. a node with the same program point. It is checked if  $s \models \Psi$ . If so,  $s$  is subsumed by  $\Psi$  meaning all paths beneath the node  $s$  would not lead to a violation of the safety property  $\Phi$ .

This, in turn, means that the key is the quality of the interpolant  $\Psi$  generated. Without interpolation, i.e. relying on state subsumption alone, is not good enough<sup>2</sup>. In Section 5, we present the *interpolation algorithm* of BACKPROP which is the main technical contribution of this paper. The BACKPROP function computes a *conjunctive approximation* of the *weakest precondition* as an interpolant.

**Remark on Depth First vs. Random Strategy:** The algorithm presented in this section is based on the depth-first traversal (DFS) of the SET. However, if the SET is so big that full coverage is implausible, then a DFS strategy in a non-pruning DSE (like KLEE) is known to have poor coverage [Cadaru et al. 2008b]. For such large programs, a *random* search strategy can be used to avoid the exploration of the SET from being stuck in some part of the SET. KLEE's "random" strategy presented in [Cadaru et al. 2008a] addresses this issue and attempts to maximize coverage.

We can utilize a random strategy in our algorithm too. This strategy would be similar to KLEE's random strategy [Cadaru et al. 2008a]. The difference between our random strategy and KLEE's random strategy is two-fold: 1) Our approach still attempts to generate path and tree-interpolants to prune the SET. 2) Our random strategy adds one more step to the two steps in KLEE's random strategy, which are executed in a round-robin fashion. This new step will pick a state which has a high chance to create a tree interpolant.

For our algorithm, the choice between DFS and random search strategies can matter greatly. DFS strategy is ideal for our algorithm since it maximizes the generation of tree-interpolants, which in turn increases the chance of subsumption. In general, in the random strategy, tree interpolant are formed slower, and memory usage is higher. On the other hand, it can reach higher coverage when the SET is not fully traversed. We follow the commonsense belief that for full exploration DFS is as good as any other strategy, whereas, for incomplete exploration, random is better. In Section 6, we will experiment with both the DFS and random strategies for our algorithm and we will show that both strategies can reach higher performance on different programs.

## 5 A PRACTICAL INTERPOLATION ALGORITHM

The essential idea behind our new interpolation algorithm is to have it be a *conjunction*. From section 3.1, we have seen that the path-based weakest precondition is in general a disjunction, hence, still not practical. So our proposed approach will entail a *conjunctive approximation* of the path-based weakest precondition. Clearly, the context itself is a first candidate. We now show that we can, by using the context as a guide, compute an effective abstraction of it.

Before we proceed, we mention abstraction learning via interpolation [Jaffar et al. 2009; McMillan 2010, 2014] which has demonstrated significant speedup in verification and testing, e.g., [Jaffar et al.

<sup>2</sup>This is because different symbolic states, that share the same program point, might be significantly different.



(1b) $\text{BACKPROP}(s, e, \Psi)$	$\equiv \Psi$	
(2b) $\text{BACKPROP}(s, x = e, \Psi)$	$\equiv \Psi[x/e]$	
(3b) $\text{BACKPROP}(s, \text{assume}(e), \text{false})$	$\equiv \neg e$	
(4b) $\text{BACKPROP}(s, \text{assume}(e), \Psi)$	$\equiv \Psi \wedge e$	if $\llbracket s \rrbracket \models e$
(5b) $\text{BACKPROP}(s, \text{assume}(e), \Psi)$	$\equiv \text{ABDUCTION}(\llbracket s \rrbracket, e, \Psi)$	otherwise

Fig. 6. Conjunctive Path-Based Weakest Precondition

2013, 2012]. Although in all of these previous efforts, the interpolants implemented are *conjunctive*, they were not as general as in the weakest precondition. In fact, all implementations ensured that an interpolant was in the form of a *conjunction* which could then be dealt with efficiently by an SMT solver.

We now present the BACKPROP function in Fig. 6 which generates a *conjunctive approximation* of the path-based weakest precondition. As before, we use the notation  $\vec{s}$  to denote a sequence of states.

Rules (1b) - (3b) are similar to the respective rules in Fig. 3. The problem at hand is to determine an interpolant which (a) it can replace  $e \implies \Psi$  from Fig. 3, and (b) it is a *conjunction*. The major difference here compared to the path-based weakest precondition (from Fig. 3) is that the rule (4a) is now replaced by the two new rules (4b) and (5b).

We first dispense the easy case in rule (4b) where  $\llbracket s \rrbracket \models e$  holds. Clearly,  $\Psi \wedge e$  is the right interpolant.

Next, we discuss the difficult case in rule (5b). We know that the best interpolant is provided by the concept of weakest precondition, that is:  $\neg e \vee \Psi$ . However, this is a disjunction, and so is not suitable for us. What we require is a general method, for generalizing the constraints, that attempt to be as powerful as the weakest precondition method. However, it is restricted to produce only a conjunction of constraints.

Note that in rule (5b), we invoke a function  $\text{ABDUCTION}(\llbracket s \rrbracket, e, \Psi)$ . We already have that  $\llbracket s \rrbracket \wedge e \models \Psi$  holds. This is by virtue of the top-down computation that brought us to this point. Now, we want a generalization  $\llbracket s \rrbracket$  such that  $\llbracket s \rrbracket \wedge e \models \Psi$ . This means we have an *abduction* problem: given a conclusion  $\Psi$  and a partial contribution  $e$  to that conclusion, what is the most general constraint needed to be added to  $e$ ? This is a classic problem [Abductive reasoning 2020]. Unfortunately, we are not aware of any general abduction algorithm that is practical for our purposes. Next, we present our own abduction algorithm.

### 5.1 The Abduction Algorithm

Consider the abduction algorithm in Fig. 7. It uses two main functions. The first is  $\text{CORE}(\gamma, \Psi)$ . The algorithm for the CORE function is presented in Fig. 7. It is called with the arguments  $\phi \wedge e$  and  $\Psi$ . Note that, as explained in the previous section, we have  $\phi \wedge e \models \Psi$ . The CORE function eliminates the constraints in  $\phi \wedge e$  that are not needed for implying  $\Psi$ . The result is stored in  $\bar{\phi}$ .

The second function is  $\text{SEPARATE}(\gamma, v)$ . The function partitions  $\gamma$  into two formulas  $\gamma_v$  and  $\gamma_{\bar{v}}$ . The algorithm stores in  $\gamma_v$ , any constraint which is either containing a variable from  $v$  or contains a variable which is appearing in another constraint in  $\gamma_v$ . The remainder of the constraints are stored in  $\gamma_{\bar{v}}$ .

The important property that is required concerns a notion of *separation*. We first define this property in general.

**Definition 5.1 (Separation).** Consider a first-order formula  $\Psi_1 \wedge \Psi_2$  where the variables of  $\Psi_1$  and  $\Psi_2$  are  $v_1$  and  $v_2$  respectively, and  $v_1$  and  $v_2$  are disjoint. Let  $\Psi_1|_{v_1}$  denote the projection of  $\Psi$  onto  $v_1$ . We say that  $\Psi_1$  and  $\Psi_2$  are *separate*, written  $\Psi_1 \star \Psi_2$ , if  $\Psi_1 \wedge \Psi_2 \equiv \Psi_1|_{v_1} \wedge \Psi_2|_{v_2}$ .  $\square$

```

ABDUCTION( $\phi, e, \Psi$ ) {      // given  $\phi \wedge e \models \Psi$ 
 $\bar{\phi} = \text{CORE}(\phi \wedge e, \Psi)$ 
  let  $v$  be the variables in  $e$ 
   $\langle \phi_v, \phi_{\bar{v}} \rangle = \text{SEPARATE}(\bar{\phi}, v)$            //  $\phi_{\bar{v}} \star (\phi_v \wedge e)$ 
  let  $v_2$  be the variables in  $(\phi_v \wedge e)$ 
   $\langle \Psi_v, \Psi_{\bar{v}} \rangle = \text{SEPARATE}(\Psi, v_2)$        //  $\Psi_{\bar{v}} \star (\phi_v \wedge e) \wedge \Psi_{\bar{v}} \star \Psi_v$ 
  if  $(\Psi_v \equiv \text{true})$  return  $\bar{\phi} \equiv \Psi_{\bar{v}}$ 
  return  $\bar{\phi} \equiv \phi_v \wedge \Psi_{\bar{v}}$ ;
}

CORE( $\gamma, \Psi$ ) {             // Assume  $\gamma$  is of the form  $C_1 \wedge \dots \wedge C_n$ 
  for  $i = 1..n$  do
    if  $\gamma - C_i \models \Psi$  then  $\gamma \equiv \gamma - C_i$ 
  return  $\gamma$ ;
}

SEPARATE( $\gamma, v$ ) {          // Assume  $\gamma$  is of the form  $C_1 \wedge \dots \wedge C_n$ 
  loop {
    oldv = v;
    for  $i = 1..n$  {
      let  $v_i$  be the variables in  $C_i$ 
      if  $v_i \cap v \neq \emptyset$  then {
         $v = v \cup v_i$ 
         $\gamma_v = \gamma_v \wedge C_i$ 
      } else  $\gamma_{\bar{v}} = \gamma_{\bar{v}} \wedge C_i$ 
    }
    until  $(v == \text{oldv})$ ; } // fixpoint condition
  return  $\langle \gamma_v, \gamma_{\bar{v}} \rangle$ ;
}

```

Fig. 7. The Abduction Algorithm

We next explain the separation property that we require from the  $\text{SEPARATE}(\gamma, v)$  function, which returns  $\gamma_v$  and  $\gamma_{\bar{v}}$ . This property is:  $\gamma_v \star \gamma_{\bar{v}}$ .

We now return to the abduction function. Note that it calls  $\text{SEPARATE}()$  twice. In the first call,  $\phi$  is partitioned into two:  $\phi_v$  and  $\phi_{\bar{v}}$ . Since,  $\text{SEPARATE}()$  is provided with the variables of  $e$ , the critical property that we would have is that the set of variables in  $(\phi_v \wedge e)$  and  $\phi_{\bar{v}}$  are disjoint. Moreover  $(\phi_v \wedge e) \star \phi_{\bar{v}}$  also holds.

In the next call,  $\Psi$  is partitioned into two. The difference here is that the  $\text{SEPARATE}()$  function is provided with the variables of  $(\phi_v \wedge e)$ . The critical property that we would have is that the set of variables in  $\Psi_v$  and  $\Psi_{\bar{v}}$  are disjoint. Moreover, the set of variables in  $(\phi_v \wedge e)$  and  $\Psi_{\bar{v}}$  are disjoint too. In the end, after the two calls to  $\text{SEPARATE}()$ , the following holds.

$$(\phi_v \wedge e) \star \phi_{\bar{v}}, \Psi_v \star \Psi_{\bar{v}} \text{ and } (\phi_v \wedge e) \star \Psi_{\bar{v}} \text{ and } \phi_v \star \Psi_v \quad (1)$$

Finally,  $\phi_v \wedge \Psi_{\bar{v}}$  is returned as a generalization of  $\phi$  such that  $\Psi_{\bar{v}} \wedge \phi_v \wedge e \models \Psi$  holds. The special case is when  $\Psi_v$  contains no constraints, i.e. it is *True*. In this case,  $\Psi_{\bar{v}}$  contains all of the constraints in  $\Psi$ . Since  $\Psi \wedge e \models \Psi$  holds obviously  $\Psi$  is returned as a generalization of  $\phi$ .

We now outline a proof that the abduction algorithm is correct. We first require some helper results.

**COROLLARY 5.2 (FRAME RULE).** *Consider three first-order formulas  $A$ ,  $B$ , and  $C$ . Then  $A \models B$  iff  $C \star A \models C \star B$ .  $\square$*

**PROOF.** That  $A \models B$  implies  $C \star A \models C \star B$  is obvious. To prove  $C \star A \models C \star B$  implies  $A \models B$ , we proceed by contradiction. Assume  $A\theta$  is true while  $B\theta$  is false for some valuation  $\theta$  on the variables of  $A$  and  $B$ . We can now extend  $\theta$  to include the variables  $C$  - call this evaluation  $\theta'$ . So  $(C \wedge A)\theta'$  implies  $(C \wedge B)\theta'$ . In case  $(C \wedge A)\theta'$  is true,  $B\theta'$  must be true. This contradicts that assumption that  $B\theta$  is false because  $\theta$  and  $\theta'$  agree on the variables of  $B$ . Similarly, in case  $(C \wedge A)\theta'$  is false, then this contradicts the assumption that  $A\theta$  is true because  $\theta$  and  $\theta'$  agree on the variables of  $A$ .  $\square$

**COROLLARY 5.3 (FRAME RULE 2).** *Consider three first-order formulas  $A$ ,  $B$ ,  $C$ . If  $A \star B \models C$ , and  $A \star C$ , then  $B \models C$ .  $\square$*

**PROOF.** We have  $A \star B \models C$ . Since  $A \star C$ , we also have  $A \star B \models A \star C$ . By the Frame Rule, we have  $B \models C$ .  $\square$

**THEOREM 5.4.** *The abduction algorithm in Fig. 7, when input with the constraints  $\phi$ ,  $e$  and  $\Psi$  where  $\phi \wedge e \models \Psi$ , outputs  $\bar{\phi}$  a generalization over  $\phi$  such that  $\phi \wedge e \models \bar{\phi} \wedge e \models \Psi$ .  $\square$*

**PROOF.** Let  $\bar{\phi}$  be  $\text{CORE}(\phi \wedge e, \Psi)$ . We prove the general case:

- |   |  |
|---|--|
| $\phi \wedge e \models \Psi$  | Given  |
| $\rightarrow \bar{\phi} \wedge e \models \Psi,$   | Correctness of $\text{CORE}()$   |
| $\rightarrow \phi_v \wedge \phi_{\bar{v}} \wedge e \models \Psi_v \wedge \Psi_{\bar{v}},$   | $\langle \phi_v, \phi_{\bar{v}} \rangle = \text{SEPARATE}(\bar{\phi}, v)$ and $\langle \Psi_v, \Psi_{\bar{v}} \rangle = \text{SEPARATE}(\Psi, v_2)$ ,<br>where $v$ and $v_2$ are the set of variables in $e$ and $(\phi_v \wedge e)$ . |
| $\rightarrow \phi_{\bar{v}} \star (\phi_v \wedge e) \models \Psi_{\bar{v}} \star \Psi_v$    | by the separation property (1).  |
| $\rightarrow (a) \phi_{\bar{v}} \star (\phi_v \wedge e) \models \Psi_{\bar{v}}$             |  |
| $\rightarrow (b) \phi_{\bar{v}} \star (\phi_v \wedge e) \models \Psi_v$                     |  |
| $\rightarrow (a') \phi_{\bar{v}} \models \Psi_{\bar{v}}$                                    | $(\phi_v \wedge e) \star \Psi_{\bar{v}}$ and Frame Rule 2  |
| $\rightarrow (b') (\phi_v \wedge e) \models \Psi_v$   | by $\phi_{\bar{v}} \star \Psi_v$ and Frame Rule 2  |
| $\rightarrow \Psi_{\bar{v}} \wedge (\phi_v \wedge e) \models \Psi_{\bar{v}} \wedge \Psi_v,$ | by $(\phi_v \wedge e) \star \Psi_{\bar{v}}$ and $\Psi_v \star \Psi_{\bar{v}}$ and the Frame Rule on $(b')$   |
| $\rightarrow \bar{\phi} \wedge e \models \Psi$  |  |

$\square$

In summary, the rule (5b) from Fig 6 performs (a) removing a constraint that already existed, or (b) transforming an existing constraint with another existing constraint. Step (a) is implemented via an unsat-core method. Step (b) on the other hand, provides a mechanism for *backward* reasoning, computing an approximation of the weakest precondition. That is, the interpolant is (partly) composed of constraints that come from the postcondition in a *bottom-up manner*, and not from the constraint of the current symbolic state, which is from a *top-down manner*.

A naive implementation of the abduction algorithm will not be sufficiently practical. We will describe how we implement the algorithm in Section 5.2.

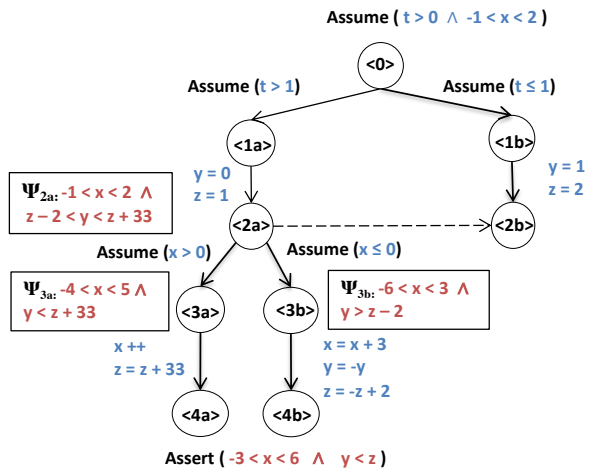


Fig. 8. Example with Interpolation

We now exemplify the concepts behind the BACKPROP algorithm in the following synthetic example. We attempt to show that first, the BACKPROP algorithm can generate a non-trivial interpolant; and second that the interpolant generated by the unsatisfiability core method is not an ideal solution, i.e. it is less general as compared to the BACKPROP algorithm.

*Example 5.5.* In Fig. 8, we depict the full SET of a program explored by DSEI. Note that program points are denoted by numbers, e.g.  $\langle 2 \rangle$ , and we attach small letters to distinguish different encounters of the same program point, e.g.  $\langle 2a \rangle$ . Assume,  $t$  and  $x$  are symbolic variables and  $y$  and  $z$  are program variables. We are attempting to prove the postcondition  $-3 < x < 6 \wedge y < z$ .

The left most path is traversed to  $\langle 4a \rangle$  and since it is safe, an interpolant  $\Psi_{3a}$  is generated at  $\langle 3a \rangle$  using rule (2b):  $-4 < x < 5 \wedge y < z + 33$ . Moving now to the path  $\langle 1 \rangle \langle 2a \rangle \langle 3b \rangle \langle 4b \rangle$ , the interpolant generated at  $\langle 3b \rangle$  using rule (2b) would be  $\Psi_{3b}$ :  $-6 < x < 3 \wedge y > z - 2$ .

We now show how to propagate  $\Psi_{3a}$  and  $\Psi_{3b}$  to obtain  $\Psi_{2a}$ . Consider first  $\Psi_{3a}$ . At  $\langle 2a \rangle$ , the guard in question is *assume*( $x > 0$ ). We apply rule (5b) and the ABDUCTION function. First,  $\phi$  would be  $-1 < x < 2 \wedge y = 0 \wedge z = 1$ , which still implies  $\Psi_{3a}$ . Next, since the guard has just the variable  $x$ ,  $\phi_x$  is  $-1 < x < 2$ , and  $\phi_{\bar{x}}$  is  $y = 0 \wedge z = 1$ . Finally,  $\Psi_x$  would be  $-4 < x < 5$  and  $\Psi_{\bar{x}}$  is  $y < z + 33$ . In other words, the first formula  $\phi_x$  is “in the frame of  $x$ ”, while  $\phi_{\bar{x}}$  is in the “anti-frame”. Thus the abduction formula  $\Psi_{2a}$  is  $-1 < x < 2 \wedge y < z + 33$ , which is obtained as a combination of the incoming context from the top (which implies  $-1 < x < 2$ ) and the formula  $\Psi_{3a}$  which come from the bottom. Repeating this method for  $\Psi_{3b}$ , our abduction algorithm produces another interpolant:  $-1 < x < 2 \wedge y > z - 2$ . Conjoining these two interpolants finally gives an interpolant  $\Psi_{2a}$ .

Now, moving to  $\langle 2b \rangle$  the constraint store implies the generated interpolant from  $\langle 2a \rangle$ . Hence, node  $\langle 2b \rangle$  is subsumed (a.k.a. pruned) and its safety is inferred from the computed interpolant. Finally, we note that a classic Unsat-core interpolant would be  $-1 < x < 2 \wedge y = 0 \wedge z = 1$  which obviously would not be able to subsume node  $\langle 2b \rangle$ .  $\square$

We now reconsider the example in Fig. 4 and show how the above interpolation algorithm would deal with this example in a great way. This time we do not constrain the precondition *Pre* (i.e. the  $b[i]$  can freely take any binary values), and the postcondition *Post* is  $-N \leq x[1] + x[2] + \dots + x[N] \leq N$  for various  $N$ . See Table 2 where we compare our algorithm against CBMC [Clarke et al. 2004] and LLBMC [Falke et al. 2013]. (KLEE only manages  $N = 24$  within timeout.) The reason for the vast superiority of our algorithm is that at any level  $i$  in the traversal, we compute just *one* interpolant:

$$-N + i \leq x[1] + x[2] + \dots + x[i] \leq N - i$$

which subsumes all states at this level which are encountered later. In other words, we have “perfect” subsumption. Note that our search tree size is linear in  $N$ .

## 5.2 Remarks on Implementation

We call our implementation TRACER-X. It is implemented on top of KLEE [Cadar et al. 2008a]. The main addition to KLEE is the implementation of interpolation. DSE with interpolation was implemented before in TRACER [Jaffar et al. 2012, 2011]. TRACER-X improves over TRACER by building on top of KLEE, and an enhanced interpolation algorithm which makes it more efficient, and able to handle LLVM [LLVM 2018], including C/C++ programs.

TRACER-X produces a new data structure called the *subsumption table*. This persistent structure is where the interpolants, which contain the subset of the path condition as well as the subset of

N	CBMC		LLBMC	Our algorithm	
	Time	Clauses	Time	Time	SET Size
20	0.11	10549	0.02	0.04	470
100	66.47	53509	2.66	0.42	2310
400	2460.98	214609	750.41	7.83	9210
500	$\infty$		1538.38	11.19	11510
1000	$\infty$		$\infty$	53.85	23010
2000	$\infty$		$\infty$	327.68	46010

Table 2. Running Example in Fig. 4 on CBMC, LLBMC and Our algorithm,  $\infty$  indicates timeout (3600 seconds)

memory regions are stored. When a new symbolic state is encountered, this table is consulted to check if the new state is subsumed by a record in the table, and hence its traversal need not continue. An entry in the table is created whenever KLEE removes a state from its worklist, which we assume to mean that KLEE has finished traversing the subtree originating from that state.

Now we explain how we implement the `CORE()` algorithm in Fig. 7. In Section 1 we explained how an SMT solver can use the optimization method of (CDCL) [Marques-Silva and Sakallah 1999]. More specifically, a core step in SMT solving is to involve a “theory solver” to solve a conjunction of constraints written for a particular theory. The CDCL method requires that the solver not only decides the satisfiability of the given conjunction. In case the result is “unsatisfiable”, the solver also indicates which portion of the conjunction is required to keep in its unsatisfiability proof. This is known as the *unsatisfiability core* of the conjunction. In its pure form, the core only contains constraints that were *already encountered*. Essentially, we employ the *unsatisfiability core* technology of the SMT solvers for a more efficient implementation of the `CORE()` function.

Next, we explain how we efficiently implement the `SEPARATE()` algorithm in Fig. 7. We have employed a light-weight syntactic partitioning to approximate the algorithm in the `SEPARATE()` function.

Now, we will briefly explain how we extend the interpolation algorithm to other LLVM instructions. For this, we keep some extra information in the interpolant or the context. First, we elaborate more on the operational semantics of the `malloc` and `free` instructions. The key difference in how we deal with the `malloc` instruction, compared to KLEE, is that instead of using a concrete address returned by a system call to `malloc`, we use a fresh symbolic variable. We also add into the path condition the constraints specifying that the newly-allocated region is separated from the domain of the old heap store and the new domain of the new heap store includes both of them.

We also have special treatment for the array operation and the GEP instruction. As an example, suppose the transition were  $a[i] = 5$  and  $\Psi$  was the formula  $*p = 5$ . We have extended rule (2b) from Fig 6 to return  $\langle M, i, 5 \rangle[p] = 5$  as the interpolant. This formula is to be understood in the array theory. That is,  $M$  is a distinguished array variable representing the (entire) heap,  $\langle M, i, 5 \rangle$  is an array expression representing the array obtained from  $M$  after the element 5 has been inserted into location  $i$ . Finally,  $\langle M, i, 5 \rangle[p]$  refers to the  $p^{th}$  element of this array expression.

In order to extend the interpolation algorithm to perform sound inter-procedural subsumption, we store the call stack in an efficient way with an interpolant. This stored call stack is later checked with the call stack at the subsumption point and subsumption is only allowed if the call stacks are identical.

## 6 EXPERIMENTAL EVALUATION

We used an Intel Core i7-6700 at 3.40 GHz Linux box (Ubuntu 16.04) with 32GB RAM. The programs in Tables 3, 4, 5, and 6 (47 programs) are from SV-COMP Verification tasks [Psyco 2017] and The Rigorous Examination of Reactive Systems Challenge (RERS) [RERS 2012]. A large subset of the test programs are industrial programs or have been used in testing and verification competitions. The raw experimental results can be accessed at [Artifacts 2020]<sup>3</sup>.

**Benchmarks Tested:** Our first set (psyco1 to psyco7) is from SV-COMP verification tasks [Psyco 2017]. These programs are generated by the PSYCO tool [Pscotool 2017] which produces interfaces using a symbolic execution and active automata learning. These programs contain complicated loops and are hard to analyze.

<sup>3</sup>Due to size limitations, we were not able to upload the raw experimental results as a supplementary material. Instead we uploaded the blinded experimental results at [Artifacts 2020]. Please note that the size after decompressing is  $> 5$  GB.

The second set is from RERS[RERS 2012] (prefixed with “P” and “m” in the tables). They are from RERS Challenge competition in years 2012, 2017, and 2019 (identified by ‘-R12’ to ‘-R19’ respectively). The programs identified with ‘P’ are from the three different categories of the 2012 competition [RERS 2012]: 1) easy/small, containing plain assignments; 2) medium/moderate, containing arithmetic operations; and 3) large/hard, containing array and data structure manipulation.

The programs ‘P3-R17\*’, ‘P2-T-R17\*’, and ‘P11-R17\*’ are from the LTL and Reachability problems of RERS 2017[RERS 2017] respectively. These programs are from the small and moderate size group and easy to hard categories. Similarly the ‘P\*-R19’ problems are from the Sequential Training Problem, RERS 2019 [RERS 2019]. The programs ‘m34\*’ and ‘m217\*’ are from Industrial Training Problems RERS 2019 and are divided into LTL, CTL, and Reachability Training Problems. Since, we have tested LTL problems from other tracks, here we focused on CTL and Reachability groups. These programs were the most difficult and complex programs in our experiment. We tagged the CTL and Reachability groups with ‘-C’ and ‘-R’, and the Arithmetic and Data Structure groups with ‘-A’ and ‘-D’. Most of the programs are originally unbounded and we have tested them with different bounds (the program name is suffixed by the bound e.g. -100 means the loop bound used was 100).

We performed two experiments.

- The main experiment is on penetration/verification.  
This experiment runs each program using *one target at a time*. We then considered a subset of the original targets called *hard targets*. These are obtained by filtering out targets which can be proved easily by state-of-the-art methods: vanilla symbolic execution for reachable targets, and static analysis for unreachable targets. We then reran the main experiment on hard targets only.
- The supplementary experiment is on testing/coverage.  
It is modeled after the TEST-COMP competition which has a “bug finding” component, and a “coverage” component. In the first part, bug finding, the task is to identify *one* target among all the targets injected in a program (performed for both all targets and hard targets).  
In the second part, the overall objective is to measure code coverage. More precisely, we measured the coverage of *basic blocks*. Each program is ran with the purpose of *full* exploration (timeout 1 hour), reporting any *memory or assertion error* detected along the way. (This is the default analysis of KLEE.) We report the block coverage for the 47 programs from SV-COMP and we also extend this experiment to GNU Coreutils benchmarks [Coreutils-6.11 2008].

In both experiments, our baselines are KLEE [Cadar et al. 2008a] and CBMC [Clarke et al. 2004], as the state-of-the-art DSE and SSE tools. In general, CBMC is not appropriate for the second experiment on coverage (because they react with an external environment). Hence, there we only compared with KLEE, and use the Coreutils benchmark.

## 6.1 Main Experiment (Penetration)

The main purpose of this experiment is to detect individually each target (bug) injected in the program. Some of these targets will be easy to reach and some are very difficult. Also, some of the targets are located in unreachable parts of the program. We compare TRACER-X and the baseline approaches on their capability in detecting easy as well as hard targets.

We determine a subset of all targets as hard targets via a filtering phase. These are obtained by filtering out targets which can be proved easily by state-of-the-art methods. We filtered out all the targets that are detected by KLEE within 5 minutes. Moreover, in a second step, we filtered out

Table 3. The results for Main Experiment (All Targets)

Benchmark	#AT	KLEE			CBMC			TracerX			#W	#L	Speedup vs KLEE	Speedup vs CBMC
		Time (min)	U	R	Time (min)	U	R	Time (min)	U	R				
psyco1-100	35	153	0	5	175	0	0	2.5	30	5	30	0	0.1	-
psyco1-500	35	152	0	5	175	0	0	48	30	5	30	0	0.0	-
psyco1-1000	35	152	0	5	175	0	0	151	0	5	0	0	0.0	-
psyco2-8	61	285	0	4	128	57	4	17	57	4	0	0	1.4	251
psyco2-10	61	285	0	4	243	57	4	107	57	4	0	0	1.3	454
psyco2-12	61	285	0	4	305	0	0	287	0	4	0	0	1.0	-
psyco3-8	61	285	0	4	124	57	4	17	57	4	0	0	1.2	248
psyco3-10	61	285	0	4	234	57	4	98	57	4	0	0	1.1	447
psyco3-12	61	285	0	4	305	0	0	287	0	4	0	0	1.0	-
psyco4-8	61	285	0	4	109	57	4	15	57	4	0	0	1.4	231
psyco4-10	61	285	0	4	245	57	4	93	57	4	0	0	1.5	474
psyco4-12	61	285	0	4	305	0	0	287	0	4	0	0	1.2	-
psyco5-100	33	141	0	5	165	0	0	2.6	28	5	28	0	0.7	-
psyco5-500	33	142	0	5	165	0	0	50	28	5	28	0	0.1	-
psyco5-1000	33	142	0	5	165	0	0	141	0	5	0	0	0.0	-
psyco6-100	47	154	0	17	235	0	0	4.5	30	17	30	0	0.3	-
psyco6-500	47	156	0	17	235	0	0	90	30	17	30	0	0.0	-
psyco6-1000	47	154	0	17	235	0	0	153	0	17	0	0	0.0	-
psyco7-8	74	381	0	0	370	0	0	10	74	0	74	0	-	-
psyco7-10	74	383	0	0	370	0	0	13	74	0	74	0	-	-
psyco7-12	74	381	0	0	370	0	0	17	74	0	74	0	-	-
m34-C-A-6	213	1013	0	13	725	133	0	15	158	55	67	0	188	31
m34-C-D-10	712	3540	0	6	3560	0	0	3162	0	102	96	0	369	-
m217-R-A-25	232	1006	0	54	1155	3	0	826	0	90	36	3	35	-
m217-R-D-3	100	443	0	12	500	0	0	12	84	16	88	0	11	-
P4-R12-8	61	300	0	1	305	0	0	36	60	1	60	0	1.1	-
P5-R12-8	61	300	0	1	305	0	0	144	36	25	60	0	0.5	-
P6-R12-8	61	293	0	3	266	35	26	99	35	26	0	0	1.8	15
P11-R19-50	190	436	0	114	30	76	114	398	0	114	0	76	9.3	13
P12-R19-10	101	287	0	46	467	8	0	174	0	67	21	8	24	-
P17-R12-8	61	184	0	25	305	0	0	183	0	25	0	0	2.2	-
P2-T-R17-12	86	192	0	51	355	23	0	3.9	35	51	12	0	94	16
P3-R17-7	164	492	0	79	820	0	0	9.9	85	79	85	0	60	-
P11-R17-7	163	503	0	68	423	91	0	7.8	95	68	4	0	-	9.5
P14-R12-20	154	468	0	70	770	0	0	37	35	119	84	0	13	-
m34-R-A-6	413	1779	0	91	1665	231	0	339	322	91	91	0	13	3.5
m217-C-A-10	32	138	1	4	0.3	0	32	3.6	0	32	0	0	228	1.6
m217-C-D-10	98	476	0	3	2.7	64	34	36	64	34	0	0	17	2.2
P1-R19-20	30	96	0	12	0.3	0	30	49	0	21	0	9	74	3.7
P2-R19-20	38	85	0	24	187	0	2	5.8	0	37	12	0	170	325
P3-R19-15	75	196	0	40	352	16	0	177	0	40	0	16	80	-
P3-R12-8	166	454	0	76	327	90	76	8.6	90	76	0	0	4.1	199
P12-R19-6	101	197	0	65	339	35	1	7.3	36	65	1	0	15	2.7
P16-R12-8	257	626	1	138	1285	0	0	54	116	141	118	0	3.3	-
P15-R12-8	223	541	0	117	1115	0	0	96	106	117	106	0	4.6	-
P1-R18-15	43	52	0	34	0.5	0	43	0.3	0	43	0	0	50	5.7
P3-R18-15	107	493	0	9	12	77	30	5.8	78	29	0	0	175	19

Table 4. The results for Main Experiment (Hard Targets)

Benchmark	#HT	KLEE			CBMC			TracerX			#W	#L	Speedup vs KLEE	Speedup vs CBMC
		Time (min)	U	R	Time (min)	U	R	Time (min)	U	R				
psyco1-100	12	120	0	0	120	0	0	0.7	12	0	12	0	-	-
psyco1-500	12	120	0	0	120	0	0	13	12	0	12	0	-	-
psyco1-1000	12	120	0	0	120	0	0	60	12	0	12	0	-	-
psyco2-8	20	200	0	0	36	20	0	4.7	20	0	0	0	-	7.6
psyco2-10	20	200	0	0	68	20	0	32	20	0	0	0	-	2.1
psyco2-12	20	203	0	0	115	20	0	200	5	0	0	15	-	0.6
psyco3-8	20	200	0	0	36	20	0	4.9	20	0	0	0	-	7.3
psyco3-10	20	200	0	0	68	20	0	33	20	0	0	0	-	2.1
psyco3-12	20	203	0	0	117	20	0	201	0	0	0	20	-	-
psyco4-8	21	210	0	0	38	21	0	4.9	21	0	0	0	-	7.7
psyco4-10	21	210	0	0	72	21	0	34	21	0	0	0	-	2.1
psyco4-12	21	212	0	0	122	21	0	207	21	0	0	0	-	0.6
psyco5-100	11	110	0	0	110	0	0	0.7	11	0	11	0	-	-
psyco5-500	11	110	0	0	110	0	0	13	11	0	11	0	-	-
psyco5-1000	11	110	0	0	110	0	0	60	11	0	11	0	-	-
psyco6-100	3	30	0	0	26	3	0	0.3	3	0	0	0	-	86
psyco6-500	3	30	0	0	30	0	0	6.0	3	0	3	0	-	-
psyco6-1000	3	30	0	0	30	0	0	29	3	0	3	0	-	-
psyco7-8	44	460	0	0	440	0	0	6.9	44	0	44	0	-	-
psyco7-10	44	464	0	0	440	0	0	9.1	44	0	44	0	-	-
psyco7-12	44	474	0	0	440	0	0	9.5	44	0	44	0	-	-
m34-C-A-6	26	260	0	0	162	14	0	1.5	17	9	12	0	-	-
m34-C-D-10	2	18	0	2	20	0	0	0.01	0	2	0	0	1869	-
m217-R-A-25	60	505	0	27	600	0	0	419	0	26	1	2	2.9	-
m217-R-D-3	88	878	0	3	880	0	0	11	84	4	85	0	81	-
P4-R12-8	60	600	0	0	600	0	0	54	60	0	60	0	-	-
P5-R12-8	60	601	0	0	600	0	0	267	36	24	60	0	-	-
P6-R12-8	56	557	0	1	217	35	21	178	35	21	0	0	4	1.5
P11-R19-50	14	140	0	0	3.2	14	0	140	0	0	0	14	-	-
P12-R19-10	27	272	0	0	178	11	0	87	11	16	16	0	-	0.2
P17-R12-8	36	360	0	0	360	0	0	152	36	0	36	0	-	-
P2-T-R17-12	9	90	0	0	46	7	0	0.9	9	0	2	0	-	38
P3-R17-7	73	731	0	0	713	12	0	6.9	73	0	61	0	-	90
P11-R17-7	44	440	0	0	73	40	0	2.8	44	0	4	0	-	13
P14-R12-20	35	354	0	0	329	24	0	21	35	0	11	0	-	15
m34-R-A-6	96	960	0	0	550	79	0	88	96	0	17	0	-	5.2
m217-C-A-10	11	110	0	0	0.08	0	11	0.05	0	11	0	0	-	1.1
m217-C-D-10	24	240	0	0	0.6	7	17	4.4	7	17	0	0	-	3.1
P1-R19-20	9	90	0	0	0.07	0	9	17	0	8	0	1	-	0.9
P2-R19-20	6	60	0	0	40	0	6	0.08	0	6	0	0	-	575
P3-R19-15	12	120	0	0	53	12	0	121	0	0	0	12	-	-
P3-R12-8	72	722	0	0	129	72	0	6.1	72	0	0	0	-	21
P12-R19-6	15	150	0	0	6.5	15	0	2.4	15	0	0	0	-	2.7
P16-R12-8	119	1181	0	1	1190	0	0	40	116	3	118	0	3.7	-
P15-R12-8	111	1061	0	5	1110	0	0	84	106	5	106	0	2.2	-
P1-R18-15	3	23	0	2	0.03	0	3	0.02	0	3	0	0	1470	3.1
P3-R18-15	9	90	0	0	1.1	5	4	0.4	5	4	0	0	-	13



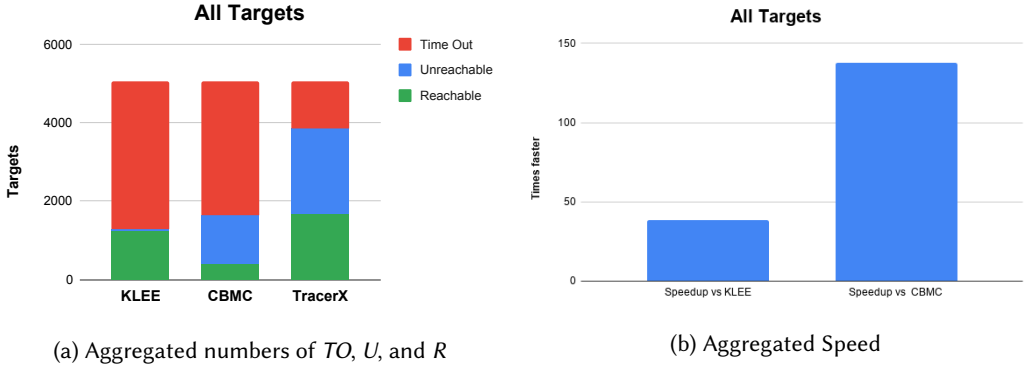


Fig. 9. Aggregated results for All target experiment

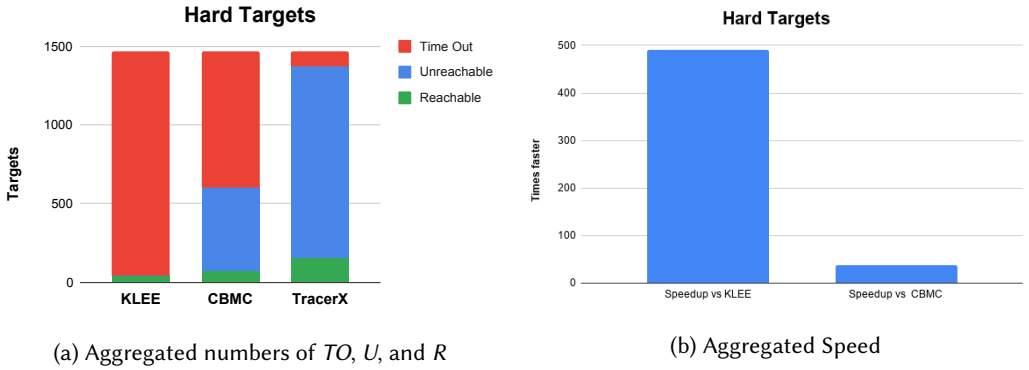


Fig. 10. Aggregated results for Hard target experiment

any target which can be determined as unreachable by Framma-C [Framma-C 2020] (a sound static analyzer). We consider the remaining targets as hard targets.

See Table 3 which presents the results of our experiment on all targets. The KLEE column reports KLEE running in its random mode [Cadaru et al. 2008a] (the choice mode for code coverage), and the CBMC column reports CBMC running in its default mode. TRACER-X column reports TRACER-X running using depth-first search (DFS). We annotated each target separately in the benchmarks and ran the tools on each of the annotated programs for 5 minutes.

The *Benchmark* column reports the benchmark program names. The *#AT* column in Table 3 reports the total number of targets<sup>4</sup>. The *Time* column for each tool reports the aggregated execution time (in minutes) for all the targets injected in a program. The columns *U* and *R* report the number of targets which have been proven to be unreachable or reachable. The tools hit timeout on the remaining targets (not able to prove them as unreachable or reachable). The remaining targets, those which caused a timeout, can be computed by  $\#AT - (U + R)$  in Table 3.

The WIN column (indicated by #W) reports the numbers of targets that TRACER-X was able to prove while none of the baseline tools were able to prove. In contrast, the LOSE column (indicated by #L) reports the numbers of targets that either of the baseline tools were able to prove while TRACER-X was not able to prove it. The last two columns (Speedup vs KLEE) and (Speedup vs CBMC) show the relative speed of TRACER-X over KLEE and CBMC respectively, over targets that

<sup>4</sup>A target means `assert(0)`, which is a runtime error.

have been proved reachable or unreachable by KLEE/CBMC and TRACER-X. When a row is marked with “-” it means one of the tools had hit timeout on all targets in that program. The value denotes the relative speedup: for example, 0.5 means TRACER-X was half as fast, and 2.0 means TRACER-X was twice as fast<sup>5</sup>.

Fig. 9 shows the aggregated results of the all targets experiment. Fig. 9a shows the total numbers of targets that each tool has been able to prove as reachable or unreachable. The remaining targets are the ones where the tools timeout. Moreover, in Fig. 9b, we present the aggregate on the relative speedup of TRACER-X over KLEE and CBMC. Finally, note that the detailed information on each target can be seen in [All-Targets 2020].

See Tables 4 which present the results of our experiment on hard targets. The columns are the same as in Table 3 except for the #HT column which reports the total number of hard targets. Since, in the previous experiments, the timeout was set to 5 minutes, for the tools to have a higher chance of finding hard targets we have extended the timeout to 10 minutes.

Fig. 10 shows the aggregated results of the Hard targets experiment. Fig. 10a shows the total number of targets that each tool has been able to prove as reachable or unreachable. The remaining targets are the ones where the tools timeout. Moreover, in Fig. 10b, we present the aggregate on the relative speedup of TRACER-X over KLEE and CBMC. Finally, we reported the detailed information on each hard target ran for all the programs in [Hard-Targets 2020].

## 6.2 Supplementary Experiment (Exploration)

### 6.2.1 Bug Finding.

Table 5 shows the results of bug finding. TRACER-X-D is our system running under a Depth First Search (DFS) strategy and TRACER-X-R with a random (KLEE-like) strategy. The column *Time* is in seconds, *1/0* shows whether the target was proven (reachable or unreachable). Here, “1” means that the target was proved reachable, and “0” shows that the target is unreachable *if there was no timeout*. For this experiment, the timeout was set to 1 hour.

Fig. 11 shows aggregated results for Table 5. The height of the bar denotes the number of “wins” for each system. A system wins when it proves a target faster than the others.

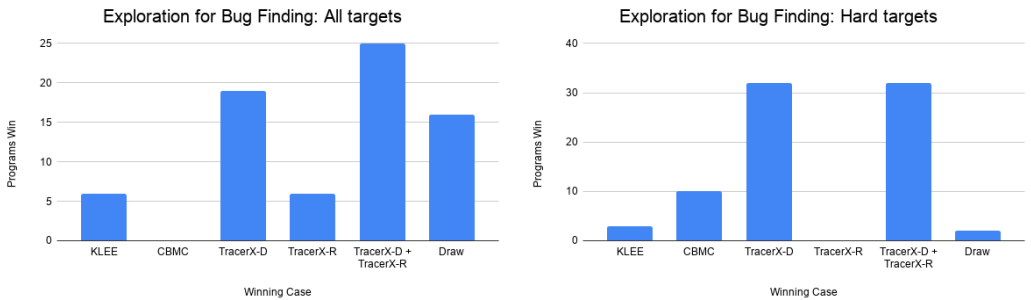


Fig. 11. Aggregated results for Bug Finding

### 6.2.2 Block Coverage.

We consider LLVM Basic Block Coverage (BB) as our coverage metric. Therefore we shall only compare against KLEE in this sub-experiment.

<sup>5</sup>The lose cases for TRACER-X have been highlighted with red color in Tables 3 and 4.

Table 5. The results for Supplementary Bug Finding Experiment (All Targets and Hard Targets)

Benchmark	All Targets								Hard Targets							
	KLEE		CBMC		TracerX-D		TracerX-R		KLEE		CBMC		TracerX-D		TracerX-R	
	Time (sec)	1/0	Time (sec)	1/0	Time (sec)	1/0	Time (sec)	1/0	Time (sec)	1/0	Time (sec)	1/0	Time (sec)	1/0	Time (sec)	1/0
psyco1-100	0.01	1	∞	0	0.22	1	0.02	1	∞	0	∞	0	5.6	0	∞	0
psyco1-500	0.02	1	∞	0	2.77	1	0.02	1	∞	0	∞	0	100	0	∞	0
psyco1-1000	0.02	1	∞	0	10.4	1	0.02	1	∞	0	∞	0	451	0	∞	0
psyco2-8	0.05	1	155	1	0.04	1	0.05	1	878	0	152	0	20	0	70	0
psyco2-10	0.03	1	295	1	0.03	1	0.03	1	∞	0	293	0	132	0	870	0
psyco2-12	0.03	1	535	1	0.04	1	0.04	1	∞	0	504	0	844	0	∞	0
psyco3-8	0.03	1	163	1	0.04	1	0.03	1	879	0	151	0	20	0	70	0
psyco3-10	0.03	1	296	1	0.04	1	0.04	1	∞	0	293	0	133	0	888	0
psyco3-12	0.03	1	520	1	0.04	1	0.03	1	∞	0	506	0	853	0	∞	0
psyco4-8	0.04	1	154	1	0.04	1	0.03	1	875	0	152	0	20	0	69	0
psyco4-10	0.03	1	306	1	0.3	1	0.03	1	∞	0	291	0	2696	0	∞	0
psyco4-12	0.03	1	518	1	0.04	1	0.03	1	∞	0	506	0	840	0	∞	0
psyco5-100	0.02	1	1893	1	0.22	1	0.02	1	∞	0	1851	0	5.8	0	∞	0
psyco5-500	0.03	1	∞	0	2.71	1	0.02	1	∞	0	∞	0	113	0	∞	0
psyco5-1000	0.02	1	∞	0	10.0	1	0.02	1	∞	0	∞	0	478	0	∞	0
psyco6-100	0.04	1	772	1	0.25	1	0.04	1	∞	0	692	0	9	0	∞	0
psyco6-500	0.04	1	∞	0	2.79	1	0.04	1	∞	0	∞	0	188	0	∞	0
psyco6-1000	0.04	1	∞	0	10.4	1	0.03	1	∞	0	∞	0	863	0	∞	0
psyco7-8	∞	0	1278	0	11.4	0	1251	0	∞	0	1280	0	11	0	1065	0
psyco7-10	∞	0	2442	0	15.7	0	1040	0	∞	0	2417	0	15	0	1185	0
psyco7-12	∞	0	∞	0	19.0	0	1820	0	∞	0	∞	0	19	0	1203	0
m34-C-A-6	0.22	1	∞	0	0.03	1	0.09	1	1973	1	∞	0	14	1	354	1
m34-C-D-10	0.31	1	∞	0	0.1	1	0.23	1	921	1	∞	0	0.5	1	155	1
m217-R-A-25	0.07	1	∞	0	0.14	1	0.06	1	410	1	∞	0	850	1	∞	0
m217-R-D-3	0.98	1	∞	0	0.11	1	0.54	1	38	1	∞	0	∞	0	189	1
P4-R12-8	0.27	1	1684	1	0.43	1	0.39	1	∞	0	1689	0	68	0	463	0
P5-R12-8	0.66	1	508	1	2.05	1	3.18	1	∞	0	545	1	271	1	1755	1
P6-R12-8	0.5	1	285	1	0.92	1	0.78	1	496	1	278	1	97	1	237	1
P11-R19-50	0.02	1	13	1	0.23	1	0.02	1	∞	0	95	0	∞	0	∞	0
P12-R19-10	0.06	1	∞	0	0.04	1	0.06	1	1018	1	∞	0	4.9	1	171	1
P17-R12-8	0.05	1	∞	0	0.24	1	0.05	1	∞	0	∞	0	821	0	∞	0
P2-T-R17-12	0.03	1	∞	0	0.03	1	0.02	1	∞	0	170	0	∞	0	∞	0
P3-R17-7	0.08	1	∞	0	0.03	1	0.08	1	∞	0	1559	0	∞	0	∞	0
P11-R17-7	0.03	1	∞	0	0.01	1	0.03	1	∞	0	∞	0	∞	0	∞	0
P14-R12-20	0.15	1	2026	1	0.33	1	0.02	1	∞	0	1877	0	167	0	∞	0
m34-R-A-6	0.22	1	∞	0	0.05	1	0.18	1	∞	0	∞	0	∞	0	∞	0
m217-C-A-10	0.22	1	6	1	0.02	1	0.1	1	849	1	4	1	0.3	1	1279	1
m217-C-D-10	0.12	1	3	1	0.03	1	0.04	1	1059	1	2	1	0.3	1	1226	1
P1-R19-20	0.02	1	1	1	0	1	0.01	1	∞	0	0.8	1	0.3	1	3131	1
P2-R19-20	0.06	1	719	1	0.04	1	0.07	1	∞	0	678	1	11	1	464	1
P3-R19-15	0.1	1	∞	0	0.05	1	0.19	1	∞	0	1463	0	∞	0	∞	0
P3-R12-8	0.02	1	178	1	0.16	1	0.02	1	∞	0	169	0	15	0	124	0
P12-R19-6	0.05	1	∞	0	0.03	1	0.06	1	2881	0	86	0	1573	0	2137	0
P16-R12-8	0.02	1	2988	1	0.13	1	0.02	1	31	1	2940	1	6	1	40	1
P15-R12-8	0.03	1	∞	0	0.13	1	0.03	1	1.58	1	∞	0	10	1	14	1
P1-R18-15	0.01	1	1	1	0	1	0.01	1	405	1	1	1	96	1	∞	0
P3-R18-15	0.02	1	7	1	0	1	0.01	1	∞	0	7	1	2	1	∞	0

Table 6 shows the results of coverage achieved on 47 SV-COMP programs. The column *BB* shows the block coverage percentage. Columns 1 and 5 show the *Benchmark* names. Columns 2 to 4 & 6 to 8 show KLEE, TRACER-X-D and TRACER-X-R. The columns *Time* in seconds. Timeout set at 1 hour (∞ in the table).

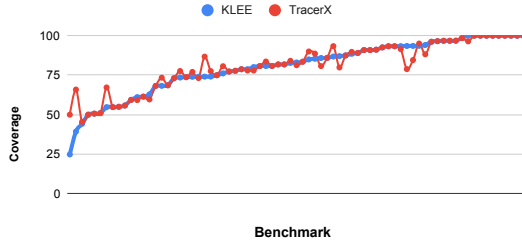
We have also experimented with the Coreutils benchmark, for which KLEE is famous for proving good coverage. For space reasons, we relegate the detailed results to the appendix, in Table 7. Instead, Fig. 12 gives an overall picture of comparison with KLEE, and also of comparison between using a DFS or random strategy.

Finally, see the aggregate results for coverage on both the SV-COMP and Coreutils benchmarks in Fig. 13.

Table 6. The results for Supplementary LLVM Block Coverage Experiment

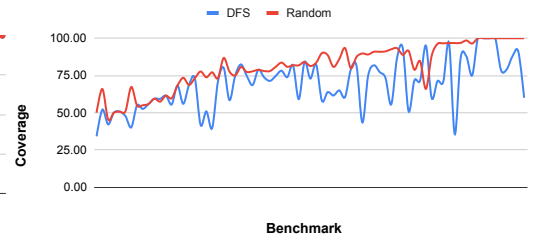
Benchmark	KLEE		TracerX-D		TracerX-R		Benchmark	KLEE		TracerX-D		TracerX-R	
	Time (sec)	BB	Time (sec)	BB	Time (sec)	BB		Time (sec)	BB	Time (sec)	BB	Time (sec)	BB
psyco2-8	845	24.53	15	24.53	55	24.53	psyco3-8	842	24.62	15	24.62	57	24.62
psyco4-8	845	24.53	15	24.53	57	24.53	P12-R19-6	2686	80.99	1229	80.99	1978	80.99
m217-R-D-3	2615	2.47	∞	1.86	∞	2.47	P3-R12-8	∞	77.23	11	77.23	122	77.23
P4-R12-8	∞	86.57	55	90.10	468	90.10	P5-R12-8	∞	77.89	295	84.03	2494	84.03
P6-R12-8	∞	79.18	254	82.46	2043	82.46	P16-R12-8	∞	76.65	54	77.11	352	77.11
psyco7-8	∞	13.79	9	16.39	1183	16.39	P15-R12-8	∞	84.27	128	84.27	1007	84.27
psyco2-10	∞	24.53	101	24.53	672	24.53	psyco3-10	∞	24.62	102	24.62	706	24.62
psyco1-100	∞	56.95	4.0	56.95	∞	56.95	psyco1-500	∞	56.95	75	56.95	∞	56.95
psyco1-1000	∞	56.95	373	56.95	∞	56.95	psyco2-B12	∞	24.53	651	24.53	∞	24.53
psyco3-B12	∞	24.62	647	24.62	∞	24.62	psyco4-10	∞	24.53	101	24.53	∞	24.53
psyco4-12	∞	24.53	642	24.53	∞	24.53	psyco5-100	∞	54.19	4.5	54.19	∞	54.19
psyco5-500	∞	54.19	82	54.19	∞	54.19	psyco5-1000	∞	54.19	400	54.19	∞	54.19
psyco6-100	∞	59.06	6.9	59.06	∞	59.06	psyco6-500	∞	59.06	136	59.06	∞	59.06
psyco6-1000	∞	59.06	722	59.06	∞	59.06	P17-R12-8	∞	83.50	653	83.59	∞	83.59
m217-C-D-10	∞	16.69	441	40.29	∞	22.45	psyco7-10	∞	13.62	12	16.39	∞	16.39
psyco7-12	∞	13.50	14	16.39	∞	16.39	P14-R12-20	∞	96.55	128	96.55	∞	96.55
P1-R19-20	∞	58.43	∞	64.79	∞	52.43	P2-R19-20	∞	82.36	∞	87.58	∞	77.76
P3-R19-15	∞	62.37	∞	62.37	∞	62.37	m217-R-A-25	∞	69.93	∞	51.80	∞	32.83
m34-C-A-6	∞	18.53	∞	25.67	∞	18.53	m34-C-D-10	∞	2.63	∞	8.36	∞	3.78
m34-R-A-6	∞	31.36	∞	11.43	∞	22.67	m217-C-A-10	∞	50.51	∞	61.62	∞	50.51
P11-R19-50	∞	82.88	∞	79.67	∞	82.88	P12-R19-10	∞	80.99	∞	80.99	∞	82.58
P2-T-R17-12	∞	65.82	∞	65.82	∞	65.82	P3-R17-7	∞	57.70	∞	55.95	∞	57.70
P11-R17-7	∞	84.78	∞	84.78	∞	84.78	P1-R18-15	∞	94.33	∞	51.27	∞	90.65
P3-R18-15	∞	18.16	∞	23.95	∞	17.50	-	-	-	-	-	-	-

## Coreutils



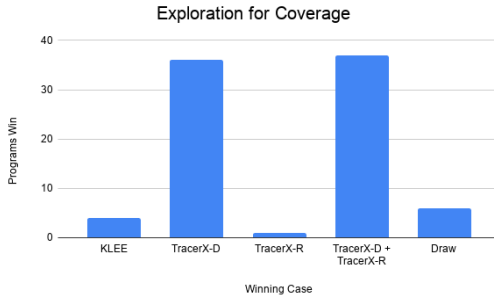
(a) KLEE vs. TracerX

## Coreutils on Tracer-X

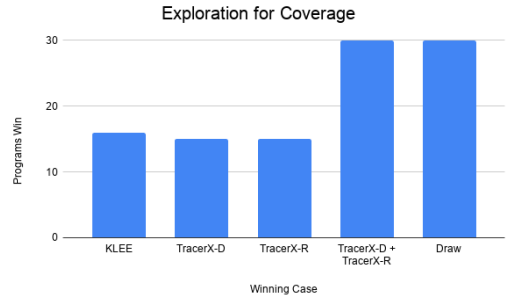


(b) TracerX-D vs. TracerX-R

Fig. 12. Analysis of Coreutils Programs



(a) Exploration of Coverage for SV-COMP programs



(b) Exploration of Coverage for Coreutils programs

Fig. 13. Aggregated results of Coverage

## 7 SUMMARY OF THE RESULTS

We now discuss the results presented above.

## 7.1 Main Experiment

Fig. 9a considered all targets. Clearly TRACER-X has superior results in terms of proving both reachable and unreachable targets; it times out less. Note that KLEE was relatively poor in proving unreachable targets, while CBMC was relatively poor for reachable targets. In the end, TRACER-X *wins* in 1339 (26.57%) targets, while *loses* in only 112 (2.21%) targets. Moving to hard targets, Fig. 10a, the gap widens. TRACER-X *wins* in 796 (54.15%) targets, while *loses* in only 64 (4.35%) targets.

In summary for the main experiment, we now present a metric *AT\_Win\_Ratio* for the final results in Tables 3 and 4. Let *AT\_Win* denote the number of TRACER-X wins, and *AT\_Lose* for losses. We define

$$AT\_Win\_Ratio\% = \frac{AT\_Win - AT\_Lose}{AT} = \frac{1339 - 112}{5058} = 24.25\%$$

to capture our performance advantage in percentage terms. Similarly, for hard targets:

$$HT\_Win\_Ratio\% = \frac{HT\_Win - HT\_Lose}{HT} = \frac{796 - 64}{1470} = 49.79\%$$

Clearly, TRACER-X is more effective as the targets become harder.

In a second comparison, we consider the relative speed of the tools. Before proceeding we mention the total time, in minutes, utilized for the three tools, TRACER-X, KLEE and CBMC was 7782, 19648 and 20105 respectively for all targets. For hard targets, the numbers are 2634, 14630 and 10630.

In Fig. 9b, we aggregate the relative speedup of TRACER-X over KLEE and CBMC. Recall that we are considering targets for which the tools terminate. Over all targets, TRACER-X is 38.55× faster than KLEE and 137.56× faster than CBMC. Also, it can be observed that KLEE and CBMC have nearly the same total time. Regarding the speed computation, for TRACER-X has in total, 33 winning programs, and 10 losing programs as compared to KLEE<sup>6</sup>. Also, TRACER-X has in total, 20 winning programs and 0 losing programs as compared to CBMC. When considering hard targets, Fig. 10b, the numbers are as follows. TRACER-X is 490.26× faster than KLEE and 37.50× faster than CBMC. TRACER-X has won in 7 winning programs and loses in no programs as compared to KLEE. Also, TRACER-X wins in 20 programs and loses in 4 programs as compared to CBMC.

## 7.2 Supplementary Experiment

We first discuss the bug-finding results. We can observe in Table 5<sup>7</sup> that KLEE found the targets easily for 44 programs out of 47 programs. KLEE timeouts on the remaining 3 programs since all the targets were unreachable. But, when we ran the same set of programs with hard targets, then KLEE timeouts on 32 programs, proves 4 programs have unreachable targets, and proves a first target as reachable for 11 programs. We can observe that KLEE struggles in proving hard targets. On the other hand, the performance of CBMC for *all* and *hard* targets experiments is almost the same except for few cases.

While in the all targets experiment KLEE outperforms CBMC, CBMC has better performance in the hard targets programs. There are some programs which are draw where two of the tools have the same performance.

Finally, we consider TRACER-X. Here, we observe that TRACER-X-D is having a good performance in nearly all the easy targets. However, in some cases, it fails to reach the performance of KLEE. In these programs, we notice that TRACER-X-R is competitive compared with KLEE. Moving to the hard targets, we observe that TRACER-X-D has a better performance compared to TRACER-X-R.

<sup>6</sup>There are some programs with 0.0 times faster, it means the time difference is very small.

<sup>7</sup>Three programs were finished very fast assume (<0.009 sec) which have been highlighted with blue color.

See Fig. 11 which presents the aggregated number of programs where each tool was able to prove in the all targets and hard targets experiments. Here, we separately compare TRACER-X-D and TRACER-X-R with the baseline tools. TRACER-X-D clearly outperforms KLEE and CBMC in both all targets and hard target experiments. In the all targets experiment, we notice that TRACER-X-R wins on nearly as many programs as KLEE. By combining TRACER-X-D and TRACER-X-R for these experiments, i.e. TRACER-X-D + TRACER-X-R, then TRACER-X has more number of winning cases and outperforms KLEE and CBMC significantly.

In summary, we conclude that TRACER-X-D has good performance on both all Targets and hard Targets categories. Also, we have noted that TRACER-X-R is competitive with KLEE and when considered it can improve the overall performance of TRACER-X.

We now discuss the coverage experiments, where we compare with only KLEE, and the set of targets is defined by the basic blocks. Fig. 13a shows the aggregated results for SV-COMP programs. It can be observed that KLEE terminated only on 5 programs and timeout on 42 programs, whereas TRACER-X-D terminated on 31 programs and TRACER-X-R terminated on 13 programs. Among the 47 programs, KLEE wins on 4 programs. There is a group where none of the systems terminated within timeout so higher *BB* will be required to compare. Here, TRACER-X-D wins on 6 programs out of 15 programs. There is 1 program for which TRACER-X-R won, and also for 2 programs TRACER-X-R has better coverage compared to TRACER-X-D but the same as KLEE. If we consider TRACER-X-D and TRACER-X-R together then our system wins on 38 programs.

We finally discuss the performances of KLEE, TRACER-X-D, and TRACER-X-R on Coreutils benchmarks. From Table 7 in the Appendix section, we can observe that TRACER-X-D terminates and is faster in 12 programs compared to KLEE. Next, in Fig. 12 on the Coreutils programs where neither KLEE nor TRACER-X terminates, we observe that KLEE has better coverage in 13 programs. Here, TRACER-X-D does not perform well because of the huge execution SET. TRACER-X-D has better coverage in only 3 programs. However, TRACER-X-R has competitive results as compared to KLEE. TRACER-X-R has better coverage on 15 programs. Moreover, in Fig. 13b we report the aggregated result on the 75 Coreutils programs. Overall, KLEE wins on 16 programs, and our combined result of TRACER-X-D + TRACER-X-R wins on 30 programs.

In summary, consider first the 47 SV-COMP programs. In bug-finding, TRACER-X wins on 25 programs considering all targets, and on 32 programs considering hard targets. In coverage, the win is 38. Finally, for the Coreutils programs, the win is 30 out of 75, with a loss of 16.

The overall conclusion of these sets of experiments is that our algorithm has *significantly improved path coverage* of DSE by means of its interpolation algorithm. Clear evidence is given by showing many targets where TRACER-X complete search while other systems cannot, or are significantly slower. When faced with an incomplete search, the result is less clear. This may be because the link between path coverage and code coverage/bug-finding is not clear. Nevertheless, our experiments do show that our algorithm is competitive or better for this purpose too.

## 8 RELATED WORK

Abstraction learning in symbolic execution has its origin in [Jaffar et al. 2009], and is also implemented in the TRACER system [Jaffar et al. 2012, 2011]. TRACER implements two interpolation techniques: using unsatisfiability core and weakest precondition (termed *postconditioned* symbolic execution in [Yi et al. 2015]). Systems that use unsatisfiability core and weakest precondition respectively include Ultimate Automizer [Heizmann et al. 2014], and a KLEE modification reported in [Yi et al. 2015]. The use of unsatisfiability core results in an interpolant that is conjunctive for a given program point and therefore requires less performance penalty in handling. In contrast, weakest precondition might be more expensive to compute, yet logically is the weakest interpolant, hence its use may result in more subsumptions.

Abstraction learning is also popularly known as *lazy annotations* (LA) in [McMillan 2010, 2014]. In [McMillan 2014] McMillan reported experiments on comparing abstraction learning with various other approaches, including *property-directed reachability* (PDR) and *bounded model checking* (BMC). He observed that PDR, as implemented in Z3 produced less effective learned annotations. On the other hand, BMC technology, e.g. [Clarke et al. 2005; Cordeiro et al. 2012; Holzer et al. 2008; LLBMC 2012 2012], employs as backend a SAT or SMT solver, hence it employs learning, however, its learning is *unstructured*, where a learned clause may come from the entire formula [McMillan 2014]. In contrast, learning in LA is structured, where an interpolant learnt is a set of facts describing a single program point.

Recently *Veritestng* [Avgerinos et al. 2016] leveraged modern SMT solvers to enhance symbolic execution for bug finding. Basically, a program is partitioned into *difficult* and *easy* fragments: the former are explored in DSE mode (i.e., KLEE mode), while the latter are explored using SSE mode with some power of pruning (i.e., BMC mode). Though this paper and *veritestng* share the same motivation, the distinction is clear. First, our learning is *structured* and has *customizable* interpolation techniques. Second, we directly address the problem of pruning in DSE mode via the use of symbolic addresses. In contrast, there will be program fragments where Veritestng's performance will downgrade to naive DSE, e.g. our motivating examples. In summary, we believe that our proposed algorithm can also be used to enhance Veritestng.

Our approach is also slightly related to various *state merging* techniques in symbolic execution, in the sense that both state merging and abstraction learning terminates a symbolic execution path prematurely while ensuring precision. State merging encodes multiple symbolic paths using *ite* expressions (disjunctions) fed into the solver. The article [Hansen et al. 2009] shows that state merging may result in significant degradation of performance, which hints that complete reliance on constraint solver for path exploration, as with the bounded model checkers (e.g., CBMC, LLBMC), may not always be the most efficient approach for symbolic execution.

Finally, there is very recent work on KLEE [Trabish et al. 2018] that exploits a dependency analysis to identify redundant code fragments that may be ignored during symbolic execution. More specifically, they execute some user-chosen functions only on-demand, using program slicing to reduce demand. This work is somewhat orthogonal to our work because of the manual input and because the slicing is a static process. In contrast, our algorithm is completely general and dynamic.

## 9 CONCLUSION

We presented a new interpolation algorithm and an implementation TRACER-X to extend KLEE with pruning. The main objective is to address the path explosion problem in pursuit of *code penetration*: to prove that a target program point is either reachable or unreachable. That is, our focus is verification. We showed via a comprehensive experimental evaluation that, while computing interpolants has a very expensive overhead, the pruning it provides often far outweighs the expense, and brings significant advantages. In the experiments, we compared against KLEE, a dynamic symbolic system with no pruning, and CBMC, a static symbolic execution system which does have pruning. We showed that our system outperforms when experimented for penetration. In fact, the performance gap widens when the verification target is harder to prove. We finally demonstrated that our system is also competitive in testing.

## REFERENCES

- Abductive reasoning. 2020. Abductive reasoning — Wikipedia, The Free Encyclopedia. [https://en.wikipedia.org/wiki/Abductive\\_reasoning](https://en.wikipedia.org/wiki/Abductive_reasoning) [Online; accessed 10-March-2020].
- All-Targets 2020. Main-Experiment-All-Targets. <https://figshare.com/s/2d6852ee9e53291c7c24>
- Artifacts 2020. Artifacts for Main and Supplementary experiments. <https://figshare.com/s/8ac010976689cab7ebd9>
- Thanassis Avgerinos, Alexandre Rebert, Sang Kil Cha, and David Brumley. 2016. Enhancing symbolic execution with veritesting. *Commun. ACM* 59, 6 (2016), 93–100.
- Cristian Cadar, Daniel Dunbar, and Dawson R Engler. 2008a. KLEE: Unassisted and Automatic Generation of High-Coverage Tests for Complex Systems Programs.. In *OSDI*. 209–224.
- Cristian Cadar, Vijay Ganesh, Peter M Pawlowski, David L Dill, and Dawson R Engler. 2008b. EXE: automatically generating inputs of death. *ACM Transactions on Information and System Security (TISSEC)* 12, 2 (2008), 10.
- Cristian Cadar and Koushik Sen. 2013. Symbolic Execution for Software Testing: Three Decades Later. *Commun. ACM* 56, 2 (2013), 82–90.
- Duc-Hiep Chu and Joxan Jaffar. 2012. A complete method for symmetry reduction in safety verification. In *CAV*. Springer, 616–633.
- Duc-Hiep Chu, Joxan Jaffar, and Rasool Maghareh. 2016. Precise Cache Timing Analysis via Symbolic Execution. In *RTAS* 2016.
- Edmund Clarke, Daniel Kroening, and Flavio Lerda. 2004. A tool for checking ANSI-C programs. In *TACAS*. Springer, 168–176.
- E. M. Clarke, D. Kroenig, N. Sharygina, and K. Yorav. 2005. SATABS: SAT-Based Predicate Abstraction for ANSI-C. In *TACAS*. 570–574.
- Lucas Cordeiro, Jeremy Morse, Denis Nicole, and Bernd Fischer. 2012. Context-bounded model checking with ESBMC 1.17. In *TACAS*. Springer, 534–537.
- Coreutils-6.11 2008. Coreutils Benchmarks (version 6.11). <https://ftp.gnu.org/gnu/coreutils/>
- Leonardo De Moura, Harald Rueß, and Maria Sorea. 2002. Lemmas on demand for satisfiability solvers. *SAT* 2 (2002), 244–251.
- Leonardo Mendonça de Moura and Nikolaj Bjørner. 2008. Proofs and Refutations, and Z3.. In *LPAR*, Vol. 418. 123–132.
- Stephan Falke, Florian Merz, and Carsten Sinz. 2013. LLBMC: improved bounded model checking of c programs using LLVM. In *TACAS*. Springer, 623–626.
- Framma-C 2020. A static analyzer. <https://frama-c.com/index.html>
- P. Godefroid, N. Klarlund, and K. Sen. 2005. DART: Directed Automated Random Testing. In *26th PLDI*. ACM Press, 213–223.
- T. Hansen, P. Schachte, and H. Søndergaard. 2009. State Joining and Splitting for the Symbolic Execution of Binaries. In *RV*. 76–92.
- Hard-Targets 2020. Main-Experiment-Hard-Targets. <https://figshare.com/s/faed7ed49aa19c25be73>
- M. Heizmann, J. Christ, D. Dietsch, J. Hoenicke, M. Lindenmann, B. Musa, C. Schilling, S. Wissert, and A. Podelski. 2014. Ultimate Automizer with Unsatisfiable Cores. In *TACAS*. 418–420.
- A. Holzer, C. Schallhart, M. Tautschnig, and H. Veith. 2008. FShell: Systematic Test Case Generation for Dynamic Analysis and Measurement. In *CAV*. 209–213.
- Joxan Jaffar, Vijayaraghavan Murali, and Jorge A Navas. 2013. Boosting concolic testing via interpolation. In *FSE*. ACM, 48–58.
- Joxan Jaffar, Vijayaraghavan Murali, Jorge A Navas, and Andrew E Santosa. 2012. TRACER: A symbolic execution tool for verification. In *CAV*. Springer, 758–766.
- J. Jaffar, J. A. Navas, and A. E. Santosa. 2011. Unbounded Symbolic Execution for Program Verification. In *RV*. 396–411.
- Joxan Jaffar, Andrew E Santosa, and Răzvan Voicu. 2009. An interpolation method for CLP traversal. In *CP*. Springer, 454–469.
- Sarfraz Khurshid, Corina S Păsăreanu, and Willem Visser. 2003. Generalized symbolic execution for model checking and testing. In *International Conference on Tools and Algorithms for the Construction and Analysis of Systems*. Springer, 553–568.
- LLBMC 2012 2012. LLBMC: Introduction. <http://llbmc.org/>
- LLVM 2018. LLVM Compiler Infrastructure Project. <https://llvm.org/>. Viewed October 2017.
- Joao P Marques-Silva and Karem A Sakallah. 1999. GRASP: A search algorithm for propositional satisfiability. *IEEE T COMPUT* 48, 5 (1999), 506–521.
- Kenneth L McMillan. 2010. Lazy Annotation for Program Testing and Verification. In *CAV*. 104–118.
- Kenneth L McMillan. 2014. Lazy Annotation Revisited. In *CAV*. 243–259.
- Psyco 2017. SV-COMP Benchmarks: Verification Tasks. <https://github.com/sosy-lab/sv-benchmarks/tree/master/c/psyco>
- Psychotool 2017. PSYCO:. <https://github.com/psycopaths/psyco>
- RERS 2012. RERS:. <http://rers-challenge.org/>



RERS 2017. RERS17:.. <http://rers-challenge.org/2017/>

RERS 2019. RERS19:.. <http://rers-challenge.org/2019/>

K. Sen, D. Marinov, and G. Agha. 2005. CUTE: a concolic unit testing engine for C. In *10th ESEC/13th SIGSOFT FSE*. ACM Press, 263–272.

David Trabish, Andrea Mattavelli, Noam Rinetzkzy, and Cristian Cadar. 2018. Chopped symbolic execution. In *ICSE*. ACM, 350–360.

Q. Yi, Z. Yang, S. Guo, C. Wang, J. Liu, and C. Zhao. 2015. Postconditioned Symbolic Execution. In *ICST*. 1–10.

## A APPENDIX

In this Appendix section, we present the detailed result of our experiments on GNU Coreutils benchmark. Table 7 has 5 major columns. Columns 1 and 2 show the *Benchmark* name and *#TB* i.e. total number of basic blocks in LLVM IR respectively. Columns 3 to 5 show results of KLEE, TRACER-X-D, and TRACER-X-R respectively. These columns further split into four sub-columns each. These sub-columns are *#Inst*, *#T*, *#VB*, and *#err*. The *#Inst* (in Millions) shows the total number of LLVM instructions covered during the exploration of the SET. *#T* (in seconds) shows the total amount of execution time consumed. The timeout we set for this experiment was 1 hour. *#VB* shows the total number of uniquely visited basic blocks. *#err* is the number of error paths traversed during the execution.

Table 7. The results of Analysis of GNU Coreutils Benchmarks

Benchmark	#TB	KLEE				TracerX-D				TracerX-R			
		#Inst	#T	#VB	#err	#Inst	#T	#VB	#err	#Inst	#T	#VB	#err
basename	51	201.0	110.23	35	0	0.5	3.92	35	0	1.5	15.81	35	0
chroot	20	29.9	18.84	15	0	1.7	9.08	15	0	3.9	19.83	15	0
cksum	52	109.8	73.85	38	0	22.9	147.24	38	0	34.4	194.18	38	0
dirname	30	55.0	35.5	15	0	0.7	6.21	15	0	3.0	17.91	15	0
printenv	33	748.5	463.82	26	0	0.9	4.03	26	0	1.5	10.39	26	0
pwd	70	2.3	1.49	43	0	0.6	1.73	43	0	0.6	2.37	43	0
runcon	75	51.5	82.99	38	0	6.4	170.76	38	0	39.9	1902.58	38	0
sync	11	1.8	1.11	9	0	0.2	0.88	9	0	0.3	1.45	9	0
uptime	62	53.5	40.84	34	0	3.0	12.14	34	0	6.9	30.18	34	0
users	32	46.9	37.06	19	0	0.9	5.76	19	0	4.9	23.54	19	0
echo	66	4344.5	$\infty$	45	0	0.5	3.75	45	0	1.7	27.16	45	0
sum	52	4618.3	$\infty$	52	0	19.4	86.07	52	0	73.2	360.86	52	0
tee	44	4604.6	$\infty$	44	0	9.7	35.97	44	0	65.5	309.17	44	0
pinky	120	1995.1	$\infty$	67	c	40.8	234.3	67	0	68.0	$\infty$	67	c
env	28	4610.7	$\infty$	28	0	22.5	65.79	28	0	133.4	$\infty$	28	0
hostname	15	1233.2	$\infty$	14	0	154.8	$\infty$	13	0	52.5	$\infty$	14	0
unlink	13	523.3	$\infty$	13	c	160.2	$\infty$	13	0	54.2	$\infty$	13	0
base64	249	11.7	$\infty$	208	0	10.6	$\infty$	205	0	39.4	$\infty$	208	0
cp	242	17.3	$\infty$	107	2	106.5	$\infty$	102	4	46.7	$\infty$	110	c
cat	119	226.9	$\infty$	106	1	37.1	$\infty$	89	9337	73.4	$\infty$	106	14964
chcon	96	398.0	$\infty$	71	0	7.1	$\infty$	38	0	33.8	$\infty$	74	c
chgrp	59	73.3	$\infty$	49	0	71.2	$\infty$	43	32	57.1	$\infty$	48	c
chmod	123	66.5	$\infty$	91	2	71.6	$\infty$	87	740	56.3	$\infty$	90	c
comm	66	861.0	$\infty$	65	0	170.1	$\infty$	58	0	94.4	$\infty$	65	c
chown	44	99.3	$\infty$	36	0	163.1	$\infty$	26	0	63.9	$\infty$	36	0
csplit	375	65.2	$\infty$	278	0	71.3	$\infty$	219	0	57.9	$\infty$	291	c
cut	201	494.7	$\infty$	188	2	144.8	$\infty$	144	1	19.4	$\infty$	170	30
date	100	23.2	$\infty$	85	0	9.0	$\infty$	58	0	33.6	$\infty$	90	c
df	209	293.3	$\infty$	182	2	104.7	$\infty$	165	1713	64.3	$\infty$	167	c
du	216	11.5	$\infty$	132	0	27.9	$\infty$	128	0	4.5	$\infty$	124	c
expand	95	1369.3	$\infty$	92	0	59.4	$\infty$	82	0	100.1	$\infty$	92	c
factor	57	6.8	$\infty$	49	0	1.3	$\infty$	37	0	2.6	$\infty$	49	0
fmt	185	100.9	$\infty$	158	0	10.6	$\infty$	118	0	93.7	$\infty$	164	c
fold	91	79.7	$\infty$	79	0	115.3	$\infty$	55	0	48.9	$\infty$	85	0
head	214	165.0	$\infty$	173	2	74.4	$\infty$	158	5	34.9	$\infty$	173	79
hostid	16	433.8	$\infty$	14	1	154.3	$\infty$	13	1	55.9	$\infty$	14	3
id	78	3093.3	$\infty$	67	c	83.1	$\infty$	48	0	72.6	$\infty$	63	c
join	385	52.2	$\infty$	311	0	44.5	$\infty$	301	0	52.6	$\infty$	322	0

Table 7 continued from previous page

kill	141	21.3	∞	132	0	63.2	∞	134	12	1.4	∞	93	0
link	14	463.6	∞	14	c	159.7	∞	11	0	87.1	∞	14	0
ln	176	183.5	∞	134	0	111.4	∞	145	0	56.8	∞	142	0
logname	11	364.1	∞	10	0	153.5	∞	9	0	57.1	∞	10	0
mkdir	28	438.1	∞	28	1	169.0	∞	21	0	70.1	∞	27	c
mkfifo	24	535.6	∞	24	1	173.4	∞	19	1594	85.1	∞	24	c
mktemp	52	357.9	∞	50	0	176.3	∞	37	0	77.7	∞	50	c
mv	108	46.4	∞	84	0	12.7	∞	74	0	52.5	∞	84	0
nice	27	32.2	∞	25	0	2.9	∞	15	0	15.4	∞	25	0
nl	102	484.6	∞	96	1	164.1	∞	61	0	93.8	∞	90	c
nohup	40	1546.1	∞	22	0	154.4	∞	21	0	75.7	∞	22	c
paste	158	149.9	∞	144	0	64.7	∞	116	0	53.5	∞	144	c
ptx	704	3.9	∞	175	0	19.7	∞	240	0	20.2	∞	352	0
readlink	31	278.3	∞	30	c	7.2	∞	30	0	40.8	∞	30	0
rm	45	235.0	∞	42	0	145.6	∞	42	0	60.6	∞	40	c
rmdir	61	72.8	∞	45	0	110.7	∞	31	0	59.3	∞	45	c
seq	106	97.8	∞	99	0	0.6	∞	54	c	6.7	∞	97	0
setuidgid	31	350.4	∞	30	0	103.1	∞	11	0	75.2	∞	30	0
shuf	136	9.8	∞	109	0	10.7	∞	97	0	4.3	∞	106	0
shred	296	25.8	∞	151	0	27.6	∞	141	0	16.0	∞	151	c
sleep	25	213.4	∞	25	0	29.7	∞	22	0	15.1	∞	25	c
sort	689	2.1	∞	271	0	2.7	∞	358	0	12.1	∞	454	0
split	166	68.2	∞	123	1	26.7	∞	133	17458	57.0	∞	144	162
stat	252	135.2	∞	172	2	24.8	∞	141	126	57.7	∞	185	61
stty	434	32.5	∞	273	0	106.6	∞	241	0	24.3	∞	259	0
tac	118	270.5	∞	93	1	4.0	∞	87	0	36.3	∞	92	0
tail	510	69.0	∞	375	2	2.9	∞	213	0	51.1	∞	396	1
touch	130	97.7	∞	105	2	5.1	∞	97	6	22.6	∞	105	79
tr	586	49.0	∞	321	0	118.5	∞	235	0	41.1	∞	394	0
tsort	123	19.1	∞	115	0	0.9	∞	88	0	6.3	∞	97	0
unexpand	116	138.8	∞	112	1	109.7	∞	82	0	71.6	∞	112	c
uniq	166	63.0	∞	147	0	6.9	∞	72	0	41.4	∞	149	0
tty	22	80.4	∞	20	0	101.1	∞	17	0	60.5	∞	20	c
who	150	234.1	∞	116	c	92.5	∞	112	0	65.4	∞	116	0
wc	151	739.6	∞	125	c	127.8	∞	127	0	50.5	∞	127	c
whoami	11	779.1	∞	11	0	160.2	∞	10	0	51.5	∞	11	0
yes	15	490.9	∞	15	0	1.5	∞	9	0	41.6	∞	15	0